

Supporting Information

to

Reversible Multi-Electron Storage in Dual-Site Redox-Active Supramolecular Cages

Raoul Plessius[†], Nicole Orth[‡], Ivana Ivanovic-Burmazovic[‡], Maxime A. Siegler[§], Joost N. H. Reek[†] and Jarl Ivar van der Vlugt[†]

[†]*University of Amsterdam, van 't Hoff Institute for Molecular Sciences, Homogeneous, Bio-Inspired and Supramolecular Catalysis Group, Science Park 904, Amsterdam, the Netherlands*

[‡]*Friedrich Alexander University Erlangen-Nuremberg, Chair of Bioinorganic Chemistry, Department of Chemistry and Pharmacy, Egerlandstrasse 1, 91058 Erlangen, Germany*

[§]*Department of Chemistry, John Hopkins University, Baltimore, Maryland 21218, United States*

Contents

General Methods.....	2
Synthesis of New Compounds.....	3
[Pd(BIAN)(pyr) ₂](OTf) ₂ (4a)	3
Pt(BIAN)Cl ₂	5
[Pt(BIAN)(OH ₂) ₂](OTf) ₂ (1b).....	7
[Pd(BIAN)(pyr) ₂](OTf) ₂ (4b)	9
BIAN-Pd Cage (3a)	11
BIAN-Pt Cage (3b)	13
Encapsulation of (B ₁₂ F ₁₂) ²⁺ as Guest.....	16
Single Crystal X-Ray Diffraction (SC-XRD)	21
Electrochemical Measurements.....	24
High-Resolution Mass Measurements	28
Electron Paramagnetic Resonance (EPR)	34
UV/Vis Spectro-Electrochemistry	35
References.....	38

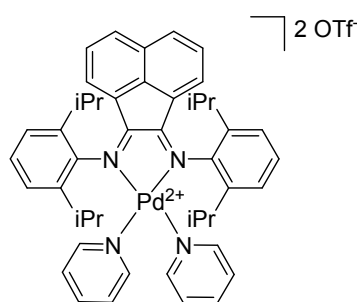
General Methods

All reactions were carried out were performed under N₂ atmosphere. With exception of the compounds given below, all reagents were purchased from commercial suppliers and used without further purification. THF, pentane, hexane, and diethyl ether were distilled from sodium benzophenone ketyl, CH₂Cl₂ and methanol from CaH₂, and toluene from sodium under N₂. NMR spectra (³¹P, ¹H and ¹³C{¹H}) were measured on a Bruker DRX 500, Bruker AMX 400, Bruker DRX 300 or on a Varian Mercury 300 NMR spectrometer at r.t. unless noted otherwise. Integration was done against residual proteated solvent (¹H, external SiMe₄ (¹³C) or external H₃PO₄ (³¹P)). 2D ¹H-DOSY measurements were performed on Bruker DRX 300 or DRX 500 NMR spectrometer with the temperature controlled at 298 K during the measurements. 2D ¹H-DOSY spectra were analysed using the Topspin software on the Bruker NMR machines. Hydrodynamic radii were calculated using the Stokes-Einstein equation.⁵¹ EPR spectra were recorded on a Bruker EMP Plus EPR spectrometer. Cyclic voltammetry measurements were performed in CH₂Cl₂ (1 × 10⁻³ M) containing N(*n*-Bu)₄PF₆ at room temperature under an N₂ atmosphere using a glassy carbon working, Ag/AgCl reference and platinum counter electrode and using a Metrohm Modular Line potentiostat. All redox potentials are referenced to Fc/Fc⁺. Spectroelectrochemistry was performed in an optically transparent thin-layer (200 μm) electrochemical (OTTLE) cell⁵² equipped with CaF₂ optical windows and a platinum mesh working electrode, which was connected to an Autolab PGSTAT302N electrochemical workstation. UV/vis spectra were recorded using a HP 8453 UV/visible spectrophotometer. All spectroelectrochemical experiments were conducted in dichloromethane containing N(*n*-Bu₄)PF₆ (0.1 M).

Trispyridyltriazine (**tpt**),⁵³ *N*¹,*N*²-bis(2,6-diisopropylphenyl)acenaphthylene-1,2-diimine ('BIAN'),⁵⁴ [Pd(BIAN)Cl₂]⁵⁵ and [Pd(BIAN)(OTf)₂]⁵⁶ were synthesized according to literature reported procedures.

Synthesis of New Compounds

[Pd(BIAN)(pyr)₂](OTf)₂ (4a)



In a 10 mL round-bottom flask, [Pd(BIAN)(OTf)₂] (100 mg, 0.11 mmol, 1 equiv.) was dissolved in 5 mL CH₂Cl₂ to obtain a bright orange solution. To this solution was added pyridine (17.9 μL, 0.22 mmol, 2 equiv.), which resulted in an instant colour change to light orange. The reaction was stirred for 1h at room temperature. Subsequently, all volatiles were removed and the target compound was obtained as a bright orange solid (95.5 mg, 81%). For analytically pure product and for electrochemical measurements, the solid was redissolved in a small amount of CH₂Cl₂ and precipitated using Et₂O. The resulting orange micro-crystalline solid was isolated by filtration in 58% yield (68.4 mg).

¹H NMR (500 MHz, CD₂Cl₂) δ 9.16 (d, *J* = 4.9 Hz, 4H), 8.25 (d, *J* = 8.3 Hz, 2H), 7.70 (t, *J* = 7.6, 1.6 Hz, 2H), 7.58 (t, *J* = 7.9 Hz, 2H), 7.45 (t, *J* = 7.8 Hz, 2H), 7.38 – 7.31 (m, 4H), 7.27 (d, *J* = 7.9 Hz, 4H), 6.47 (d, *J* = 7.4 Hz, 2H), 3.75 (p, *J* = 6.7 Hz, 4H), 1.47 (d, *J* = 6.6 Hz, 12H), 0.93 (d, *J* = 6.6 Hz, 12H).

¹³C NMR (126 MHz, CD₂Cl₂) δ 179.96, 152.17, 149.28, 140.91, 139.52, 135.06, 131.84, 131.13, 129.87, 128.42, 127.42, 125.96, 124.34, 30.01, 25.35, 23.93.

MS (*m/z*) calcd for C₄₇H₅₀F₃N₄O₃PdS: 913,2607, found 913,2613 [M-OTf]⁺.

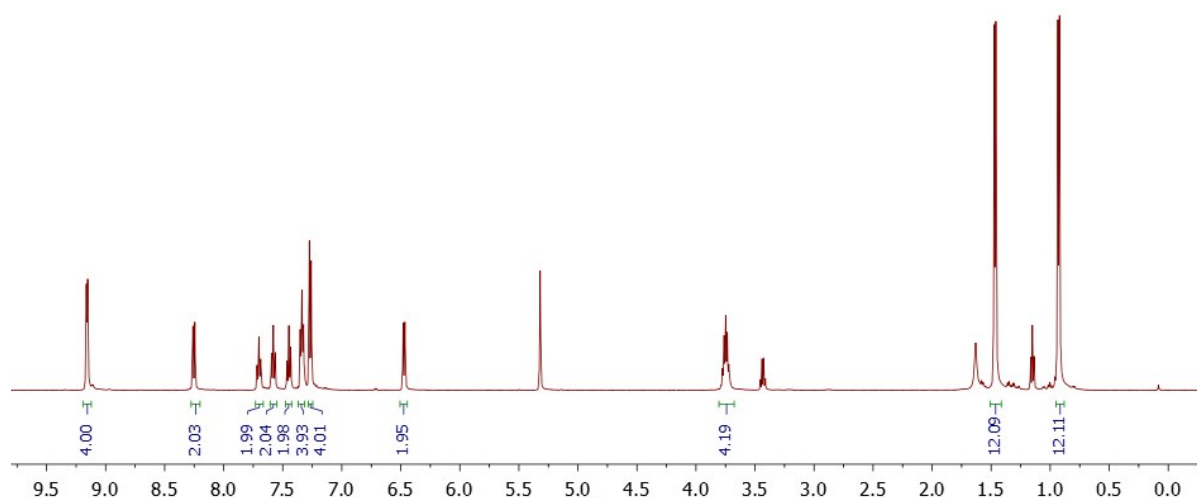


Figure S1 ¹H NMR spectrum of [Pd(BIAN)(pyr)₂](OTf)₂ in CD₂Cl₂.

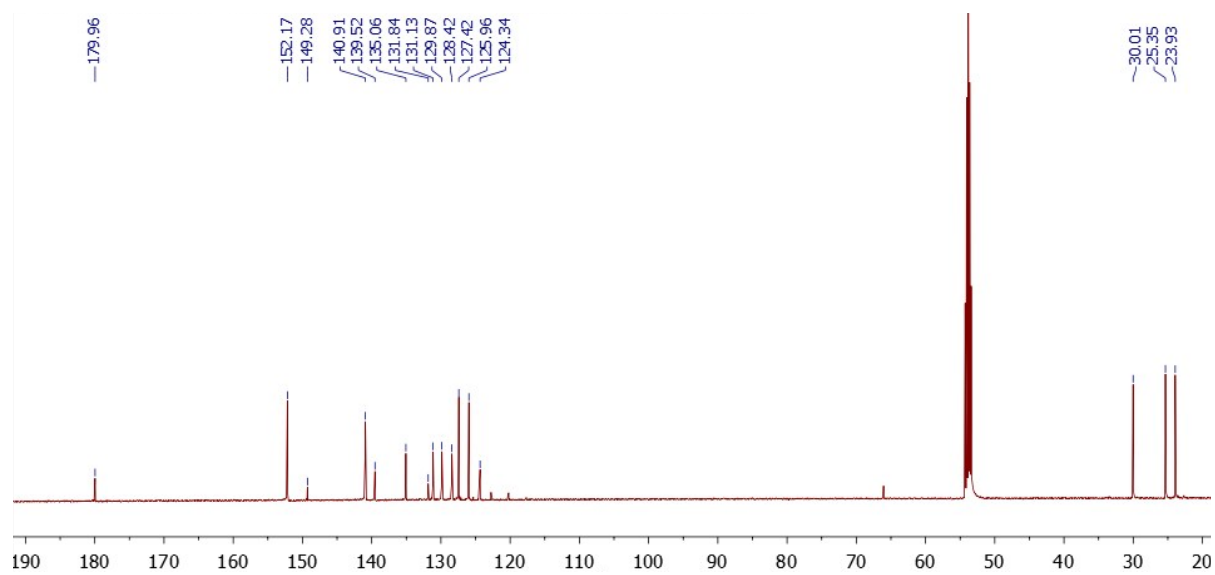


Figure S2 ^{13}C NMR spectrum of $[\text{Pd}(\text{BIAN})(\text{pyr})_2](\text{OTf})_2$ in CD_2Cl_2 .

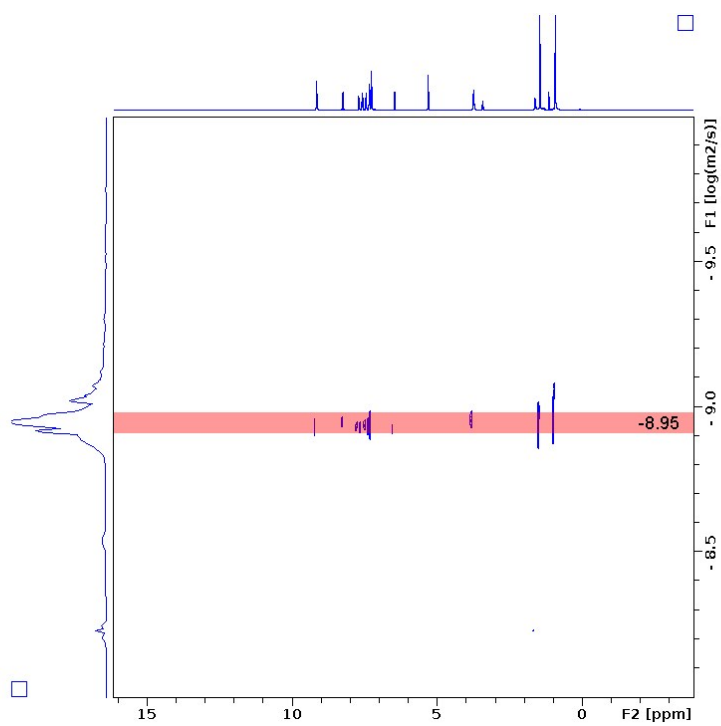
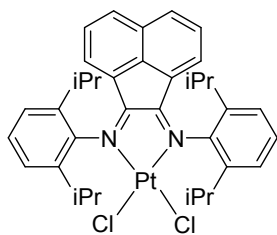


Figure S3 ^1H DOSY NMR spectrum of $\text{Pd}(\text{BIAN})(\text{pyr})_2$ in CD_2Cl_2 .

Pt(BIAN)Cl₂



The compound was synthesized according to a literature procedure,⁵⁵ but using 2,5-diisopropylphenyl side groups instead of phenyls in the report. To a clear yellow solution of K[PtCl₃(C₂H₄)] (200 mg, 0.54 mmol, 1 equiv.) in 6.5 mL MeOH was added a clear orange solution of the organic ligand 'BIAN' (277 mg, 0.55 mmol, 1.02 equiv.) under stirring. The reaction mixture immediately turned deep purple. The solution was stirred for 20 min at room temperature before Norit was added. The suspension was filtered and the residue washed with CH₂Cl₂ (approx. 10 mL). All volatiles were removed *in vacuo* and the resulting purplish-black solid was suspended in a minimum amount of Et₂O and isolated by filtration. After drying the solid *in vacuo*, the target compound was obtained as a micro-crystalline deep purple solid in 93% yield (386 mg).

¹H NMR (300 MHz, CDCl₃) δ 8.28 (d, *J* = 8.3 Hz, 2H), 7.63 – 7.50 (m, 2H), 7.41 (d, *J* = 8.0 Hz, 6H), 6.68 (d, *J* = 7.3 Hz, 2H), 3.96 – 3.20 (m, 4H), 1.48 (d, *J* = 6.8 Hz, 12H), 0.96 (d, 12H).

¹³C NMR (75 MHz, CDCl₃) δ 175.81, 146.46, 140.95, 140.68, 132.25, 131.09, 129.83, 129.51, 126.52, 124.32, 124.11, 28.85, 23.97, 23.68.

MS (*m/z*) calcd for C₃₆H₄₀Cl₂N₂Pt: 766,22087, found: 766,27885 [M⁺]

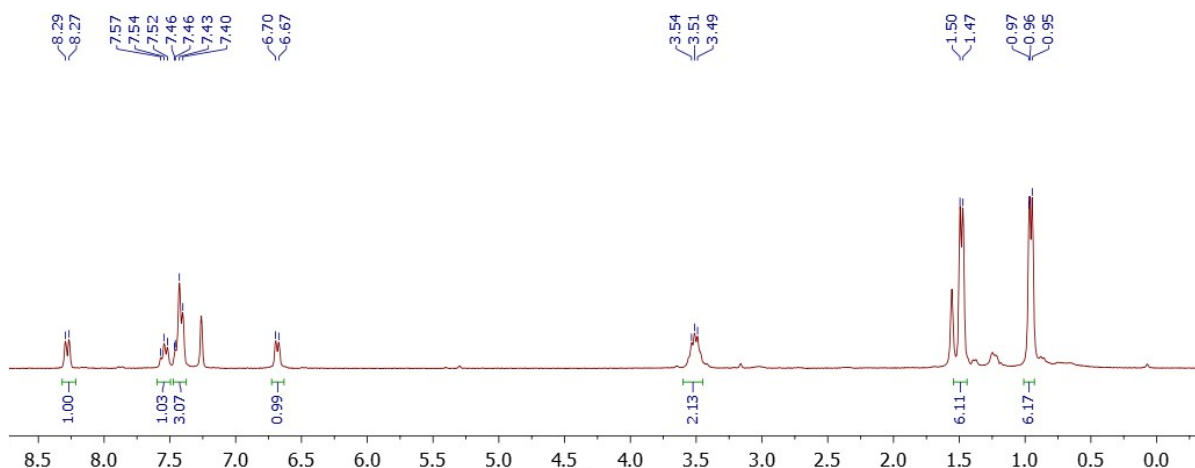


Figure S4 ¹H NMR spectrum of [Pt(BIAN)Cl₂] in CDCl₃.

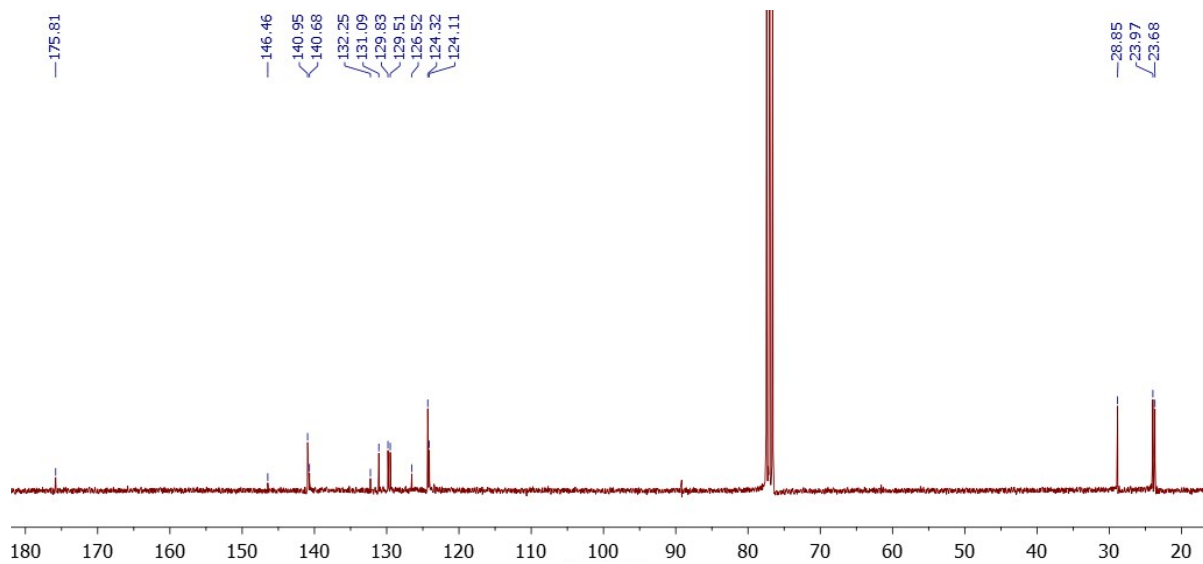
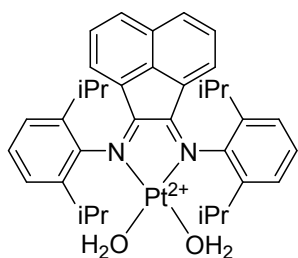


Figure S5 ^{13}C NMR spectrum of $[\text{Pt}(\text{BIAN})\text{Cl}_2]$ in CDCl_3 .

[Pt(BIAN)(OH₂)₂](OTf)₂ (1b)

To a flame-dried 50 mL Schlenk was added Pt(BIAN)Cl₂ (120 mg, 0.15 mmol, 1 equiv.) and AgOTf (114 mg, 0.44 mmol, 2.84 equiv.) as solids. The Schlenk was evacuated and refilled with N₂ three times before 10 mL dry DCM was added. After stirring overnight whilst the solution was shielded from light by wrapping the flask in aluminium foil, the light brown suspension was syringe filtered and the filtrate was stirred in air overnight. All volatiles were removed *in vacuo*, the resulting solid was dissolved in a small amount of CH₂Cl₂ and the compound precipitated using Et₂O. The target product was isolated by filtration to obtain a light brown solid in 76% yield (118 mg).

¹H NMR (300 MHz, CD₂Cl₂) δ 8.38 (d, *J* = 8.3 Hz, 2H), 7.70 (t, *J* = 7.8 Hz, 2H), 7.89 (br s, 4H), 7.65 – 7.58 (m, 2H), 7.50 (d, *J* = 7.8 Hz, 4H), 3.48 – 3.39 (m, 6H), 1.52 (d, *J* = 6.8 Hz, 12H), 1.04 (d, *J* = 6.8 Hz, 12H).

¹³C NMR (126 MHz, CD₂Cl₂) δ 180.59, 149.89, 141.13, 137.82, 134.14, 132.09, 131.26, 130.21, 126.33, 125.43, 123.18, 29.56, 23.67, 23.25.

MS (*m/z*) calcd for C₃₇H₄₀F₃N₂O₃PtS: 843,2360, found: 843.25888 [M-H -2H₂O -OTf]⁺.

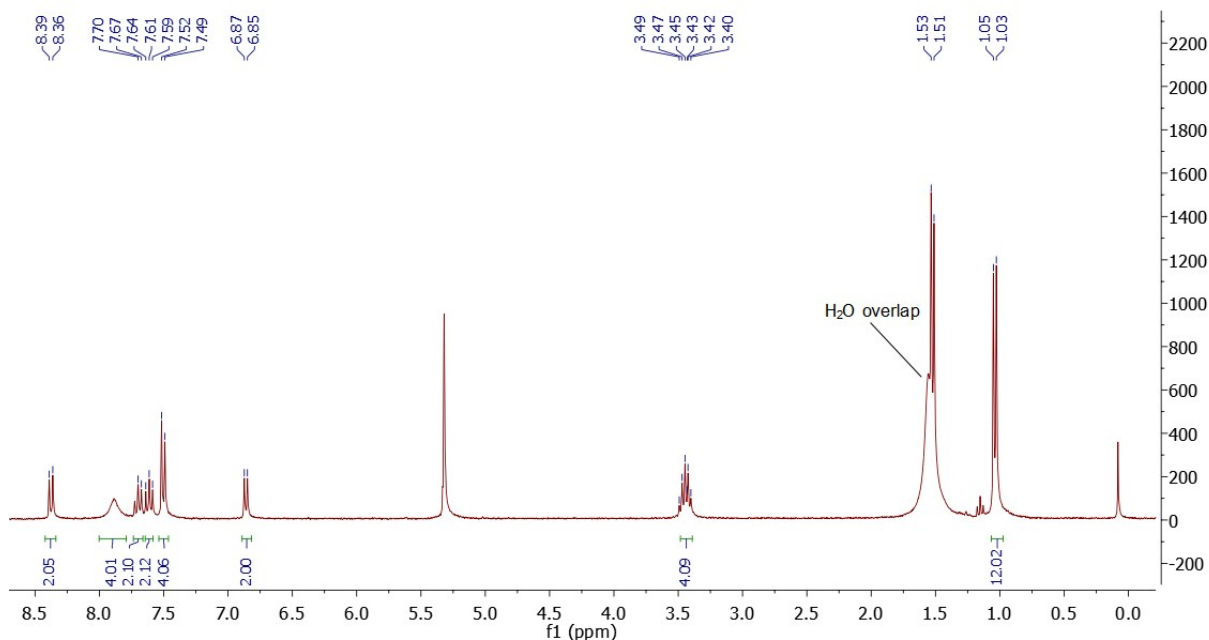


Figure S6 ¹H NMR spectrum of [Pt(BIAN)(OH₂)₂](OTf)₂ in CD₂Cl₂. Label added to signal at 1.5 ppm and integral removed.

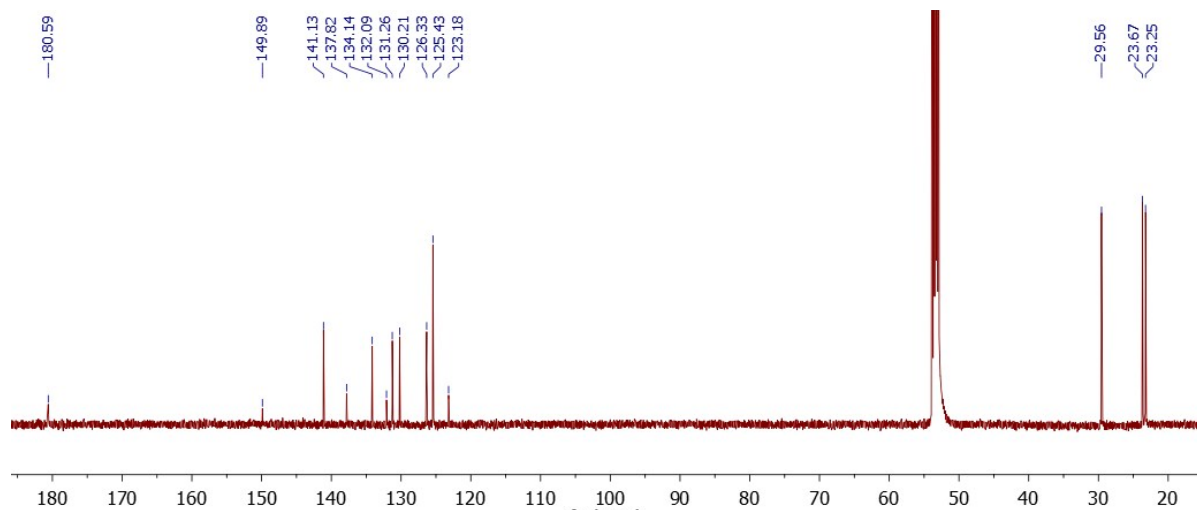
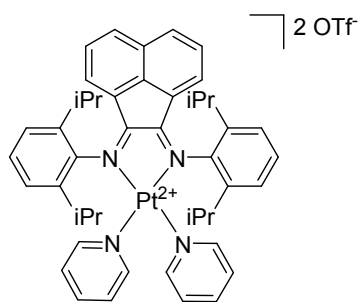


Figure S7 ^{13}C NMR spectrum of $[\text{Pt}(\text{BIAN})(\text{OH}_2)_2](\text{OTf})_2$ in CD_2Cl_2 .

[Pd(BIAN)(pyr)₂](OTf)₂ (**4b**)



In a screw-cap vial, **1b** (50 mg, 50.3 μmol , 1 equiv.) was dissolved in 4 mL CH_2Cl_2 to obtain a light brown suspension. To this mixture was added a 2 mL CH_2Cl_2 solution of pyridine (8.1 μL , 100.6 μmol , 2 equiv.), which resulted in an instant colour change to black. The vial was tightly closed, placed in a 40 $^\circ\text{C}$ oil bath and stirred for 6 hours. All volatiles were removed *in vacuo* from the clear brown reaction mixture, obtaining a brown solid as the product (55.9 mg 96%). For analytically pure product and for electrochemical measurements, the solid was redissolved in 1.5 mL CH_2Cl_2 , placed in a jar containing pentane (vapour diffusion set-up) and stored in a freezer at -20 $^\circ\text{C}$ for three days. The resulting brown micro-crystalline solid was isolated in 73% yield (42.5 mg) after filtration.

^1H NMR (300 MHz, CD_2Cl_2) δ 9.11 (d, $J = 5.9$ Hz, 4H), 8.36 (d, $J = 8.4$ Hz, 2H), 7.71 (t, $J = 7.8$ Hz, 2H), 7.60 (t, $J = 7.9$ Hz, 2H), 7.48 (t, $J = 7.8$ Hz, 2H), 7.39 – 7.25 (m, 8H), 6.64 (d, $J = 7.4$ Hz, 2H), 3.68 (p, $J = 6.8$ Hz, 4H), 1.47 (d, $J = 6.7$ Hz, 12H), 0.93 (d, $J = 6.8$ Hz, 12H).

^{13}C NMR (75 MHz, CD_2Cl_2) δ 180.44, 153.00, 149.78, 141.28, 141.13, 138.73, 134.84, 132.31, 131.40, 130.38, 127.75, 127.68, 126.06, 29.71, 25.26, 23.83.

MS (m/z) calcd for $\text{C}_{46}\text{H}_{50}\text{N}_4\text{Pt}$: 853,3683199, found: 853,37617 [$\text{M}-2\text{OTf}$] $^+$.

MS (m/z) calcd for $\text{C}_{47}\text{H}_{50}\text{F}_3\text{N}_4\text{O}_3\text{PtS}$: 1002,320363, found: 1002,32657 [$\text{M}-\text{OTf}$] $^+$.

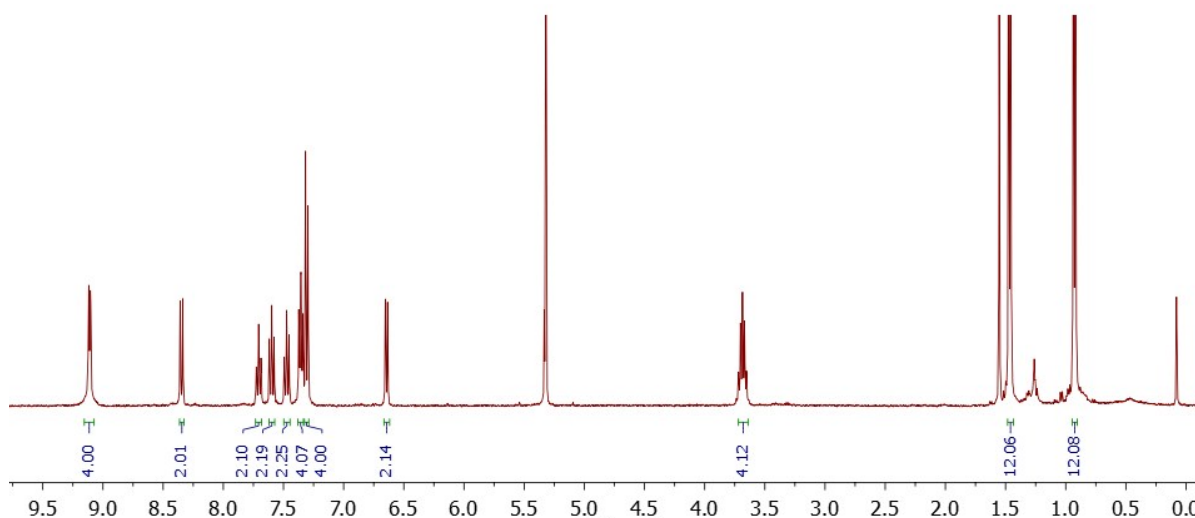


Figure S8 ^1H NMR spectrum of $[\text{Pt}(\text{BIAN})(\text{pyr})_2](\text{OTf})_2$ in CD_2Cl_2 .

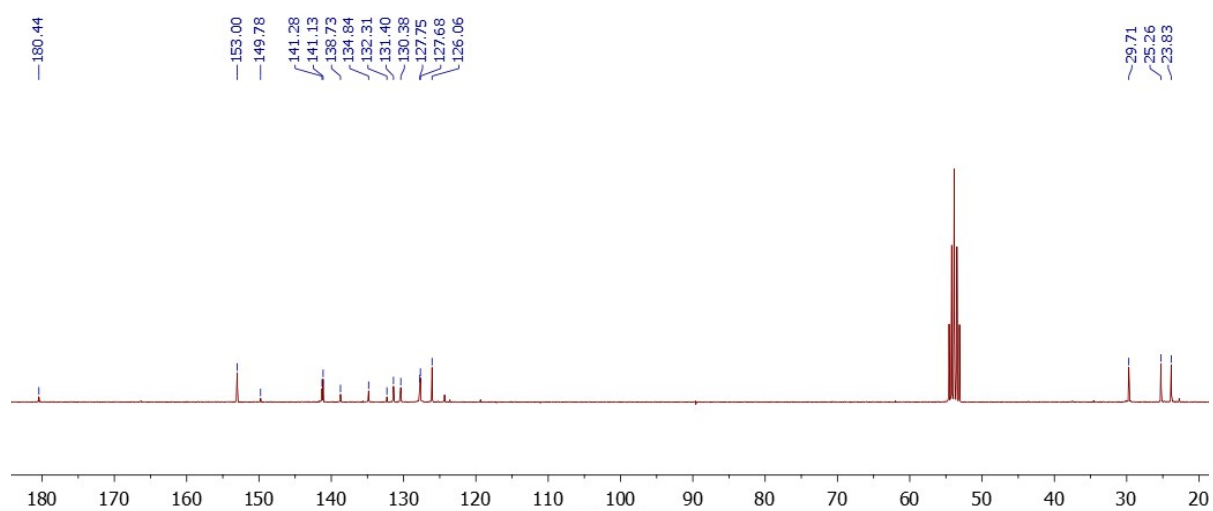
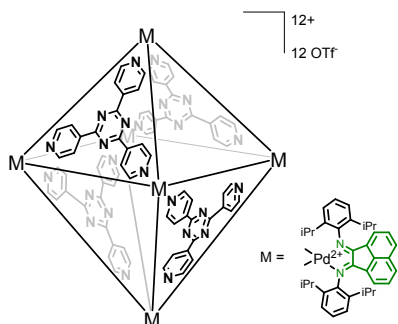


Figure S9 ^{13}C NMR spectrum of $[\text{Pt}(\text{BIAN})(\text{pyr})_2](\text{OTf})_2$ in CD_2Cl_2 .

BIAN-Pd Cage (3a)



To a screw-cap vial was added **1a** (250 mg, 0.28 mmol, 6 equiv.), *para*-trispyridyltriazine **tpt** (57.5 mg, 0.18 mmol, 4 equiv.) and 5 mL non-dried CH₂Cl₂. A bright orange suspension was obtained, which was stirred at room temperature for 16 hours. The resulting clear orange solution was diluted with approximately 4 mL non-dried CH₂Cl₂. This solution was then stored inside a container with pentane (vapour diffusion set-up) in a freezer at -

20 °C. After approximately three days, orange needles of the target compound were obtained, which were isolated by decanting off the clear faint yellow solution and washing several times with fresh pentane until the solution was colourless. The needles were dried *in vacuo* to obtain the target compound as bright orange needles (87%, 269 mg).

Vapour diffusion of 2-methyl tetrahydrofuran into a 1,2-dichloroethane solution of **3a** (at -20 °C) yielded single crystals suitable for single crystal X-ray diffraction (Figure S31). Although full refinement could not be obtained due to severe disorder in the triflate anions, the data unequivocally corroborate the anticipated connectivity and overall octahedral geometry of **3a**, with the coordination environment around each square planar Pd-ion satisfied by two pyridine N-donors and one bidentate BIAN-ligand.

¹H NMR (300 MHz, CD₂Cl₂) δ 9.16 (d, *J* = 6.0 Hz, 24H), 8.40 (d, *J* = 6.4 Hz, 24H), 8.32 (d, *J* = 8.3 Hz, 12H), 7.65 (t, *J* = 7.9 Hz, 12H), 7.49 (t, *J* = 7.8 Hz, 12H), 7.31 (d, *J* = 7.8 Hz, 24H), 6.62 (d, *J* = 7.4 Hz, 12H), 3.75 (septet, *J* = 6.6 Hz, 24H), 1.53 (d, *J* = 6.7 Hz, 96H), 1.01 (d, *J* = 6.6 Hz, 96H).

¹³C NMR (75 MHz, CD₂Cl₂) δ 181.07, 169.67, 152.63, 149.85, 145.75, 140.79, 139.65, 135.59, 131.98, 131.62, 130.06, 128.62, 126.54, 126.24, 124.02, 30.20, 25.35, 24.17.

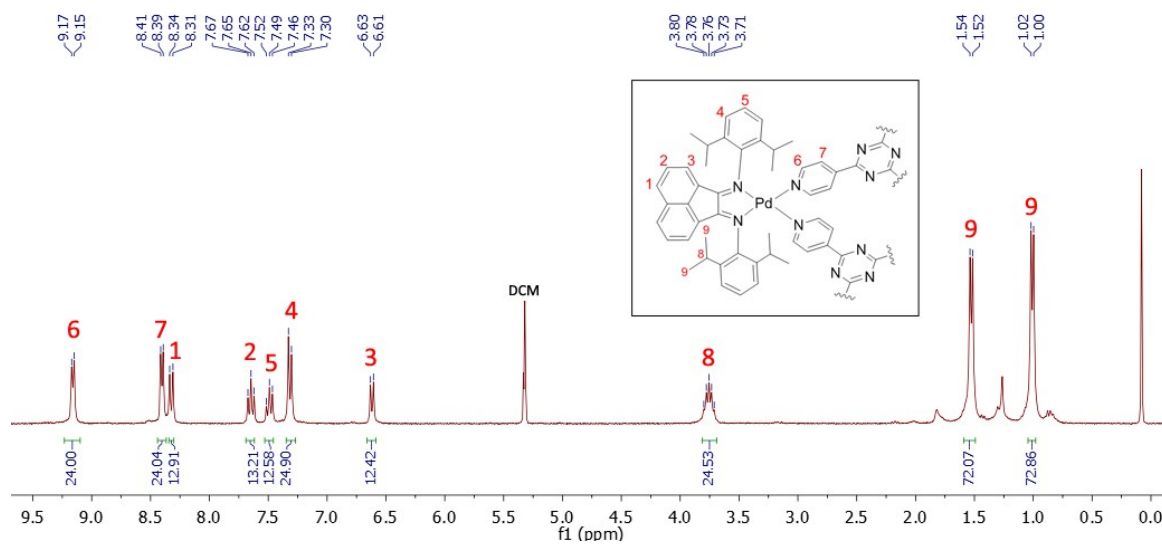


Figure S10 ^1H NMR spectrum of **3a** in CD_2Cl_2 . Attributed signals in figure.

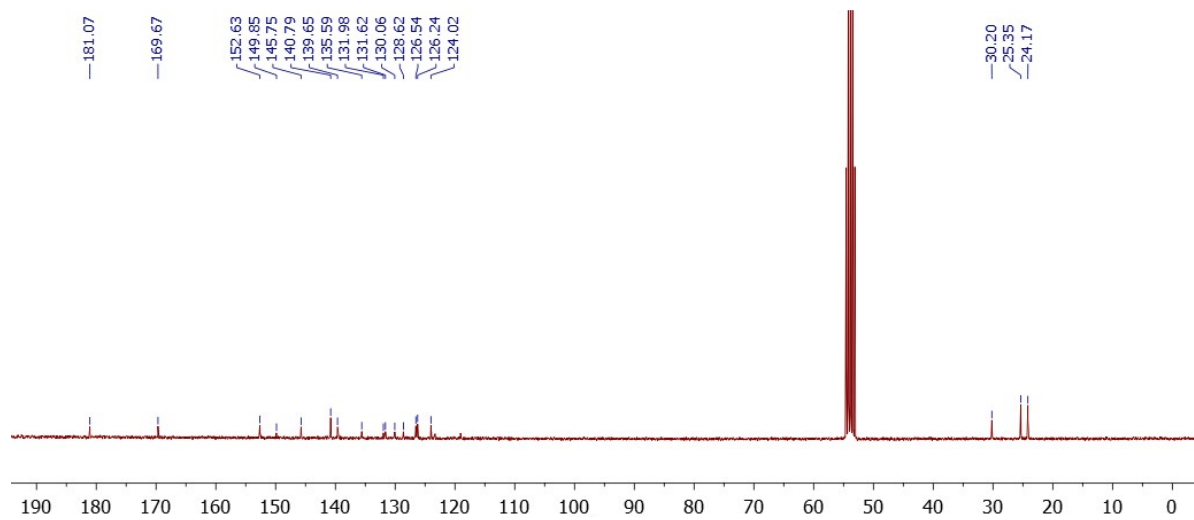


Figure S11 ^{13}C NMR spectrum of **3a** in CD_2Cl_2 .

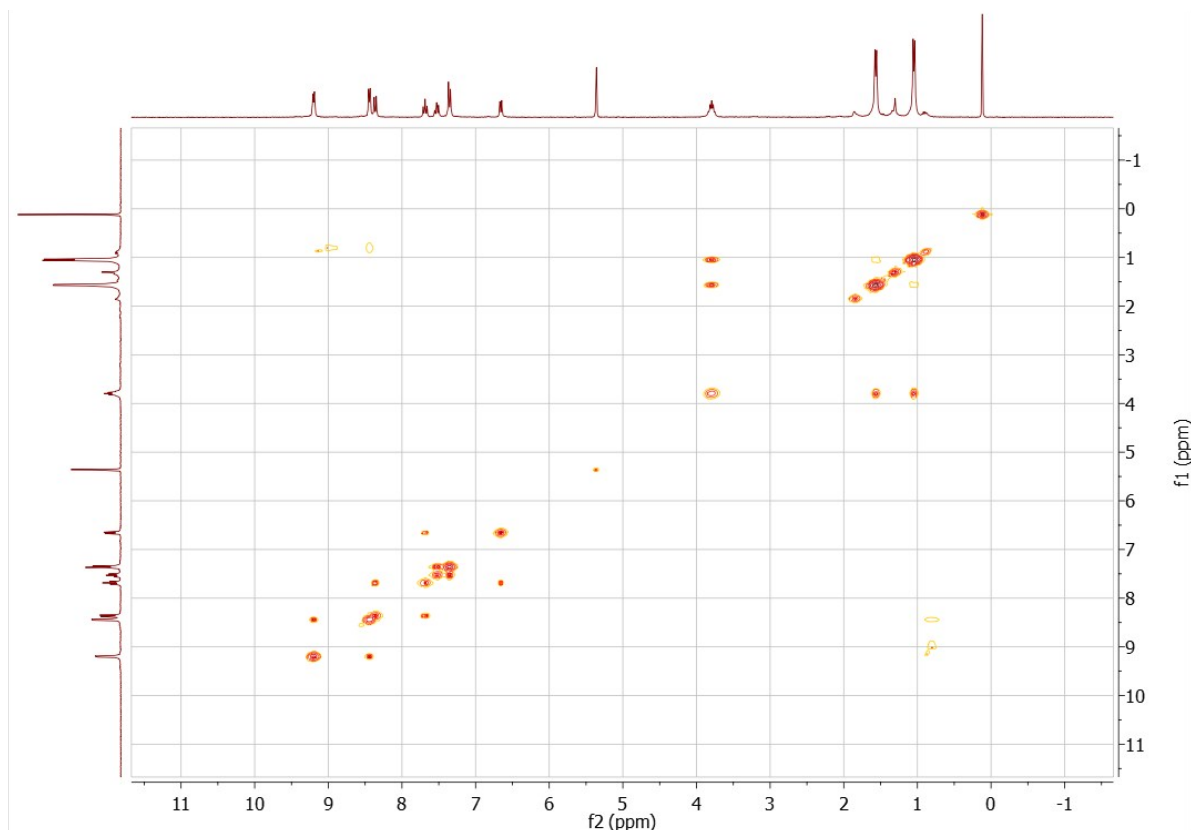


Figure S12 ^1H - ^1H COSY NMR spectrum of **3a** in CD_2Cl_2 .

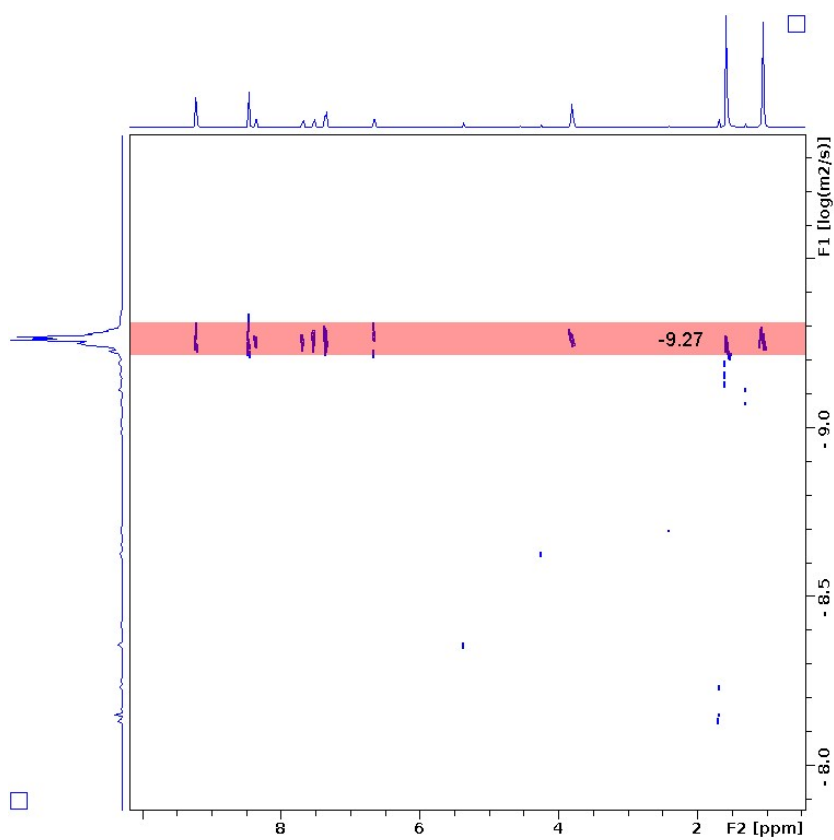


Figure S13 ^1H DOSY NMR spectrum of **3a** in CD_2Cl_2 .

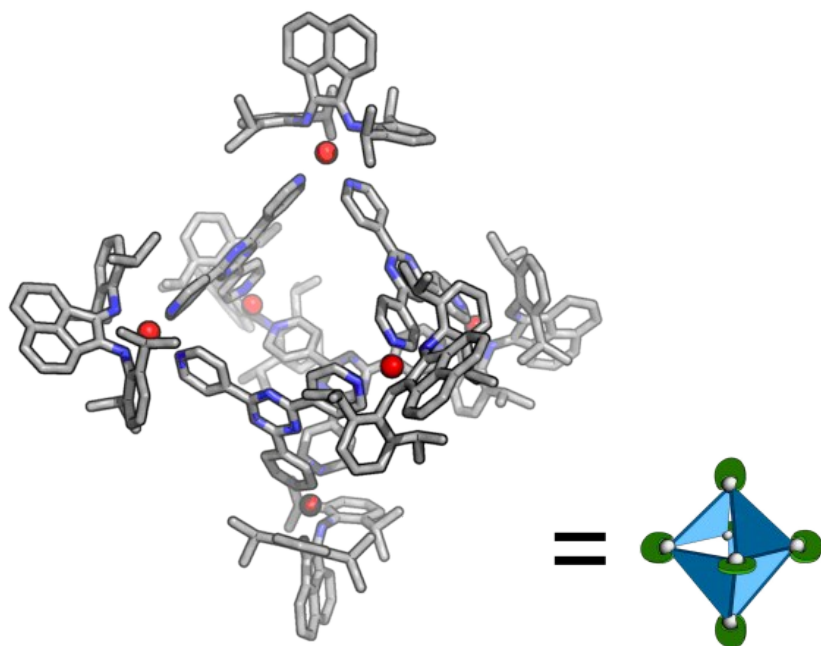
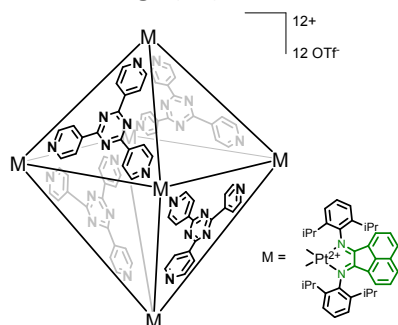


Figure S14 Connectivity plot of **3a**, obtained from X-ray diffraction. Solvent, counterions and hydrogens are omitted for clarity. Pd = red, carbon = grey, nitrogen = blue.

BIAN-Pt Cage (**3b**)



To a screw-cap vial was added **1b** (75 mg, 75.5 μmol , 6 equiv.), *para*-trispyridyltriazine (15.7 mg, 50.3 μmol , 4 equiv.), 4 mL CH_2Cl_2 and 0.67 mL MeCN. The screw-cap vial containing the red-brown suspension was tightly closed, placed in a 40 $^\circ\text{C}$ oil bath and stirred for at least 72 hours. The resulting red-brown solution was allowed to cool to room temperature, syringe filtered,

solvents removed *in vacuo* and the resulting residu redissolved in 1-2 mL CH_2Cl_2 . This solution was then stored inside a container with Et_2O (vapour diffusion set-up) in a freezer at -20 $^\circ\text{C}$. After approximately three days the container was allowed to warm to room temperature to yield a brown solid after decanting off the clear faintly yellow solution and washing several times with fresh Et_2O until the solution was colourless. The product was dried *in vacuo* and isolated as a brown solid (83%, 75.3 mg).

^1H NMR (300 MHz, CD_2Cl_2) δ 9.16 (d, J = 6.1 Hz, 24H), 8.53 (d, J = 6.7 Hz, 24H), 8.41 (d, J = 8.3 Hz, 12H), 7.66 (t, J = 7.9 Hz, 12), 7.48 (d, J = 7.7 Hz, 12H), 7.35 (d, J = 7.8 Hz, 24H), 6.75 (d, J = 7.4 Hz, 12H), 3.68 (m, J = 6.6 Hz, 24H), 1.54 (d, J = 6.6 Hz, 72H), 1.00 (d, J = 6.6 Hz, 72H).

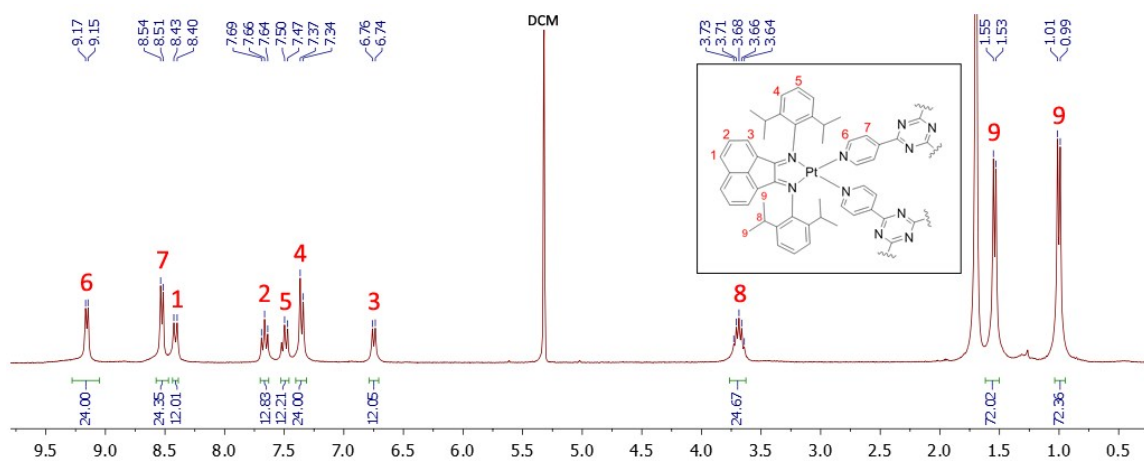


Figure S15 ^1H NMR spectrum of **3b** in CD_2Cl_2 . Attributed signals in figure.

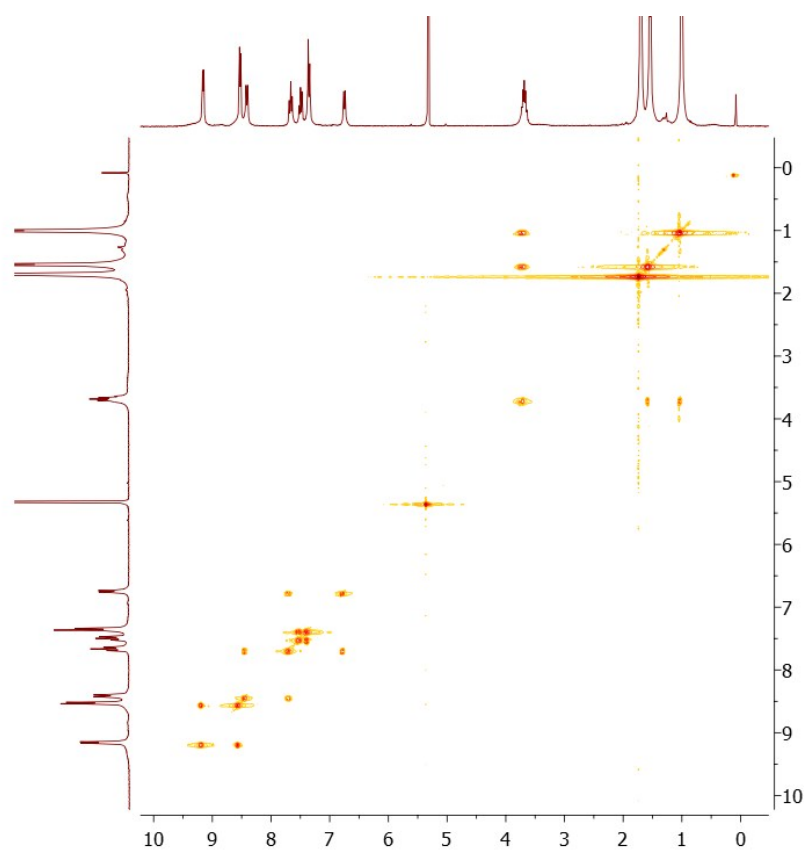


Figure S16 ^1H - ^1H COSY NMR spectrum of **3b** in CD_2Cl_2 .

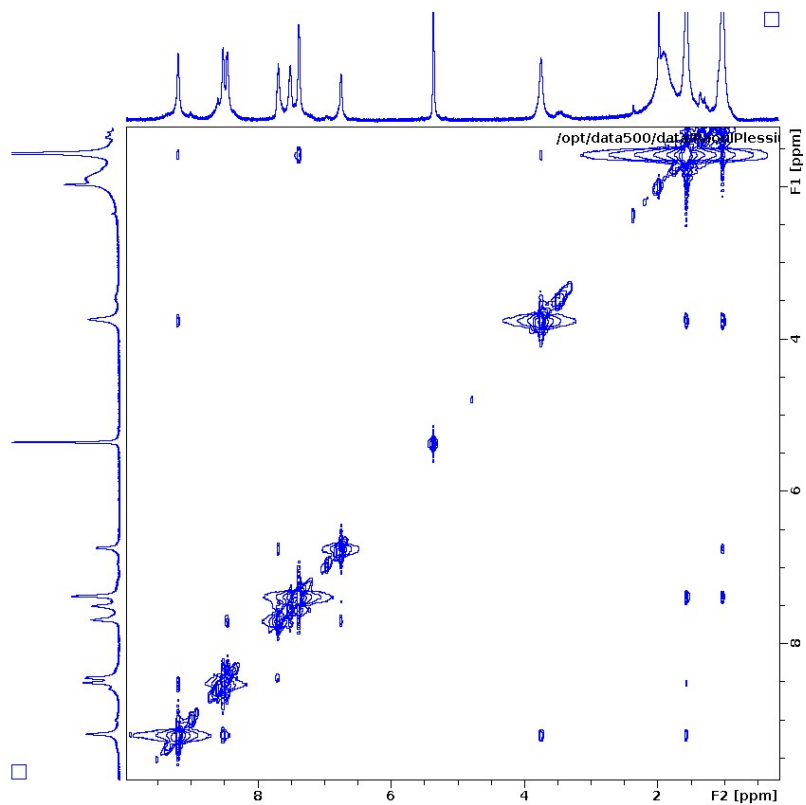


Figure S17 ^1H NOESY NMR spectrum of **3b** in $\text{CD}_2\text{Cl}_2 + \text{CD}_3\text{CN}$.

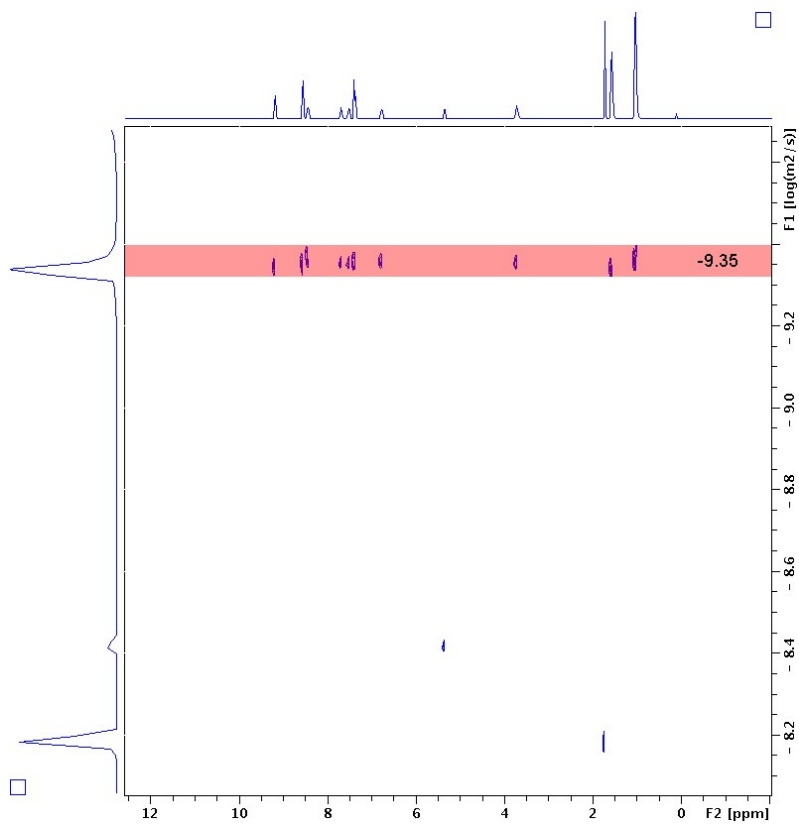


Figure S18 ^1H DOSY NMR spectrum of **3b** in CD_2Cl_2 .

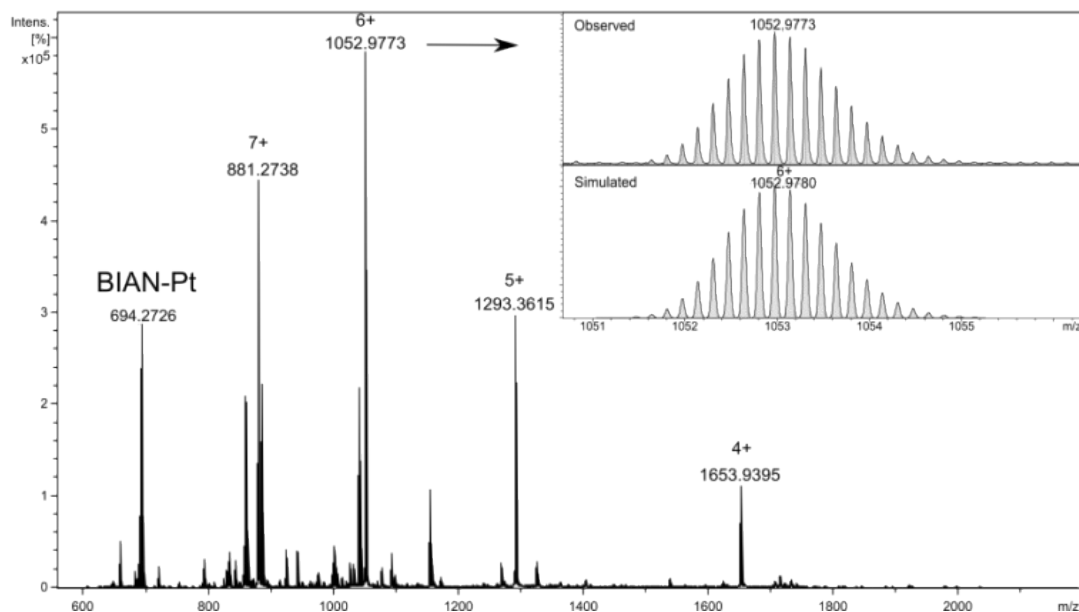


Figure S19 High resolution CSI MS spectrum of BIAN-Pt cage **3b** [Pt₆(BIAN)₆(tpt)₄](OTf)₁₂. Inset: zoom-in of the 6+ species together with relevant simulated spectrum.

Encapsulation of (B₁₂F₁₂)²⁻ as Guest

The B₁₂F₁₂²⁻ guest was used as its tetrabutylammonium salt (TBA⁺) and prepared using the following procedure:

Solid CsB₁₂F₁₂ (30 mg, 48 μmol, 1 equiv.) was suspended in 3 mL H₂O, and the suspension was heated for a couple of minutes until the mixture was fully dissolved. To this solution, solid TBABr (155 mg, 48 μmol, 10 equiv.) was added, which resulted in immediate formation of a white suspension. The mixture was sonicated for 10 minutes, followed by filtration over Celite and thorough washing with H₂O to remove the excess TBABr. The remaining white solid was extracted using DCM and the organic solvent was removed *in vacuo*. The final product was obtained as a white solid that was dried over P₂O₅ overnight. The obtained product (74%, 29.9 mg) was used without further purification. ¹⁹F and ¹¹B NMR measurements matched that of literature.⁵⁷

For encapsulation studies, 0.75 μmol of either palladium or platinum cage was dissolved in approximately 0.6 mL CD₂Cl₂. To this clear solution, one equivalent (0.75 μmol) of (TBA)₂B₁₂F₁₂ was added as a solid at room temperature. NMR spectra were measured directly after addition. Desymmetrization and broadening of the pyridyl-signals was observed (8.5 – 9.5 ppm). In addition, the ¹⁹F DOSY shows a diffusion coefficient of Log(D) = -9.35, corresponding to that of the cage.

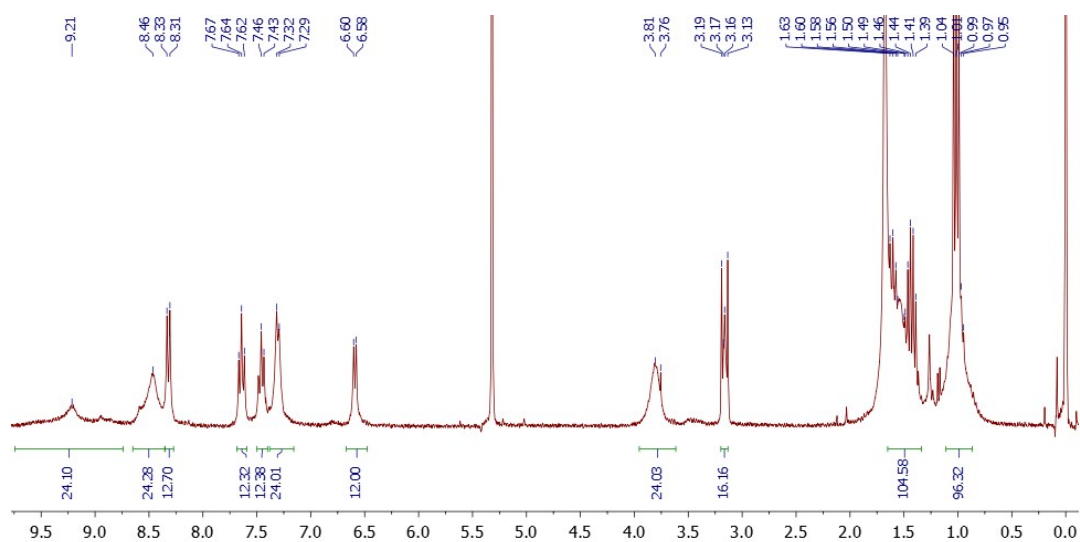


Figure S20 ^1H NMR spectrum of **3a** with one equivalent of $(\text{TBA})_2\text{B}_{12}\text{F}_{12}$ in CD_2Cl_2 .

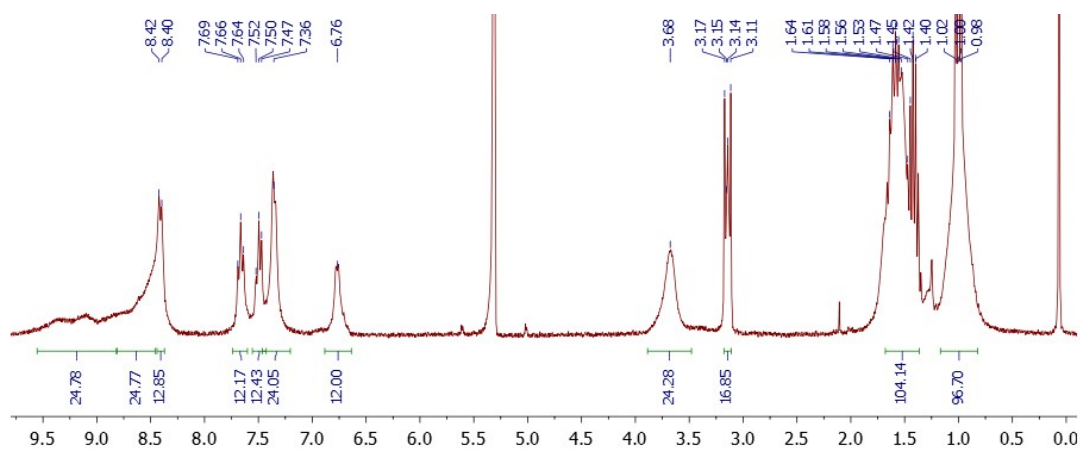


Figure S21 ^1H NMR spectrum of **3b** with one equivalent of $(\text{TBA})_2\text{B}_{12}\text{F}_{12}$ in CD_2Cl_2 .

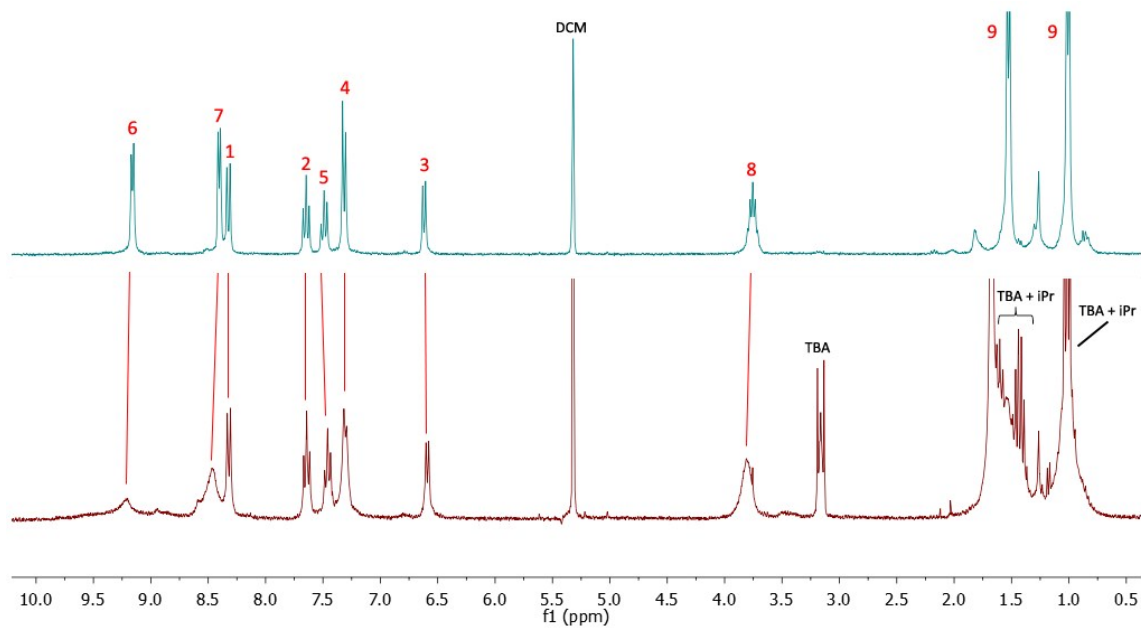


Figure S22 Top: ^1H NMR spectrum of empty BIAN-Pd cage (**3a**) in CD_2Cl_2 . Bottom: ^1H NMR spectrum of **3a** with one equivalent of $(\text{TBA})_2\text{B}_{12}\text{F}_{12}$ in CD_2Cl_2 . This figure is added, attributed signals to empty cage (**3a**) and stacked with cage+guest.

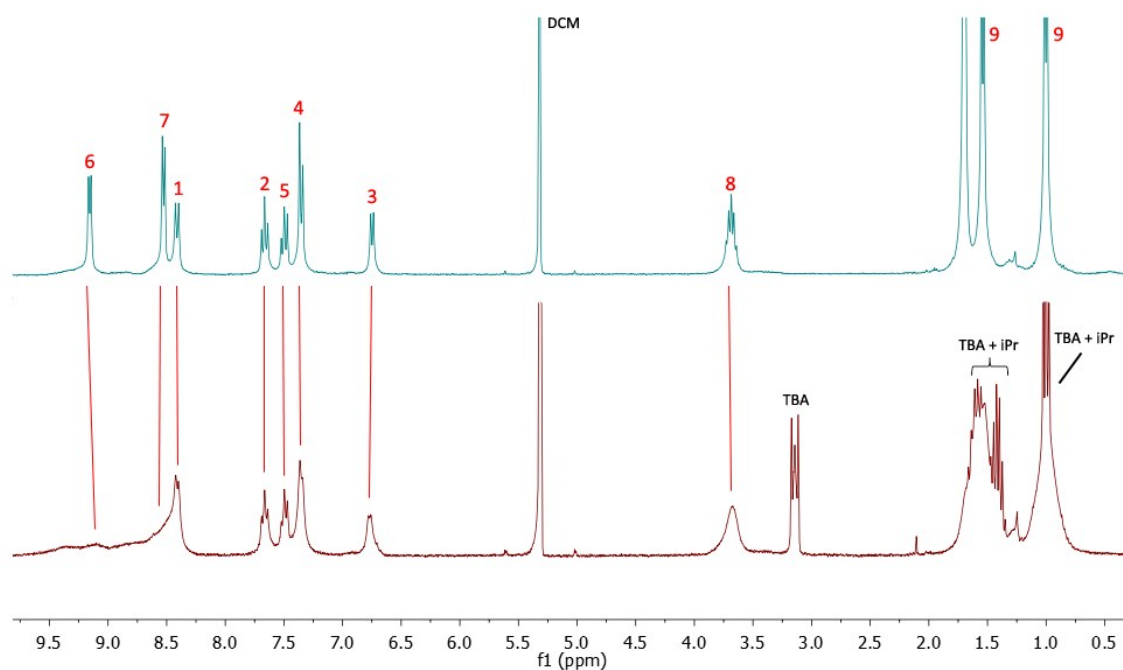


Figure S23 Top: ^1H NMR spectrum of empty BIAN-Pt cage (**3b**) in CD_2Cl_2 . Bottom: ^1H NMR spectrum of **3b** with one equivalent of $(\text{TBA})_2\text{B}_{12}\text{F}_{12}$ in CD_2Cl_2 . This figure is added, attributed signals to empty cage (**3b**) and stacked with cage+guest.

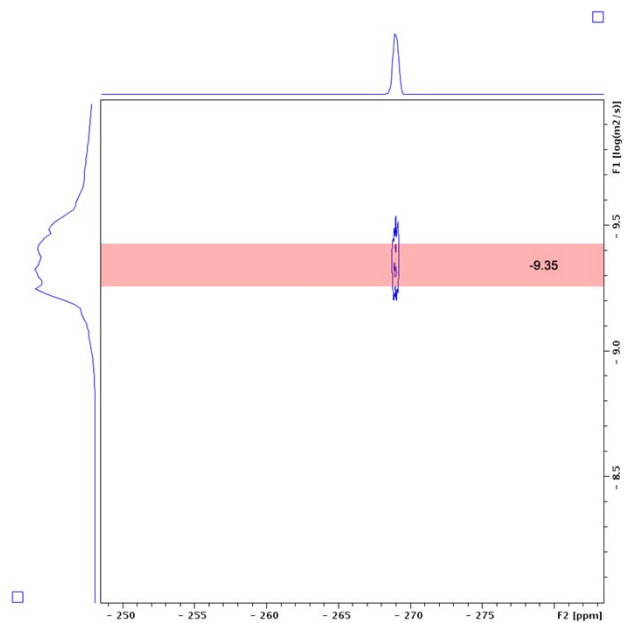


Figure S24 ¹⁹F DOSY on **3a** with one equivalent of (TBA)₂B₁₂F₁₂ in CD₂Cl₂.

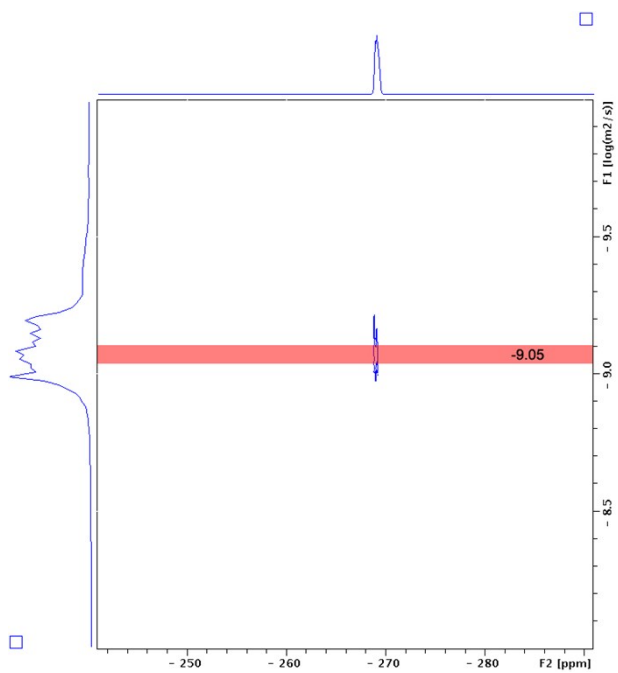


Figure S25 ¹⁹F DOSY on free (TBA)₂B₁₂F₁₂ in CD₂Cl₂.

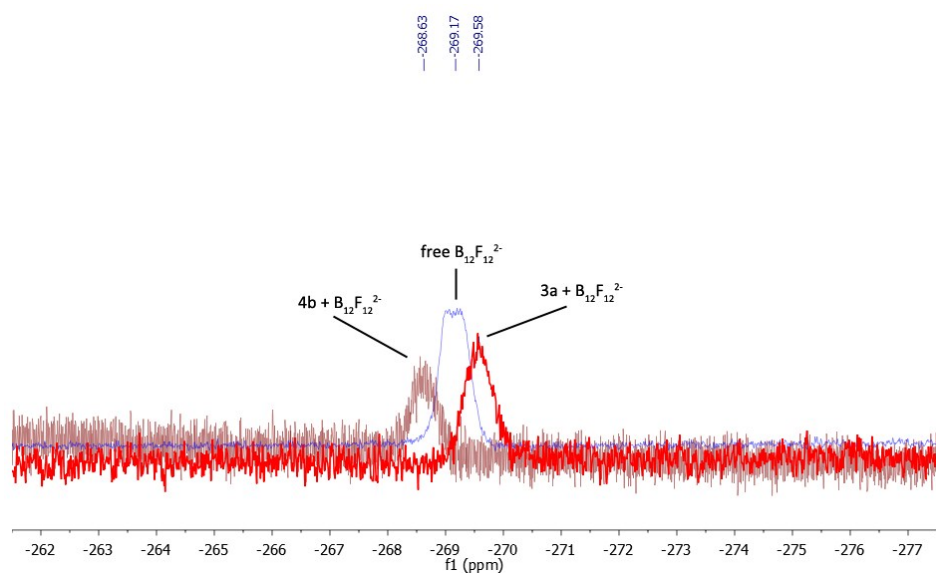


Figure S26 ^{19}F NMR spectra of model compound **4b** (maroon trace) with $(\text{TBA})_2\text{B}_{12}\text{F}_{12}$, free $(\text{TBA})_2\text{B}_{12}\text{F}_{12}$ (blue trace) and **3a** (red trace) with one equivalent of $(\text{TBA})_2\text{B}_{12}\text{F}_{12}$ in CD_2Cl_2 at room temperature. All spectra have been internally referenced to the signal of (OTf).

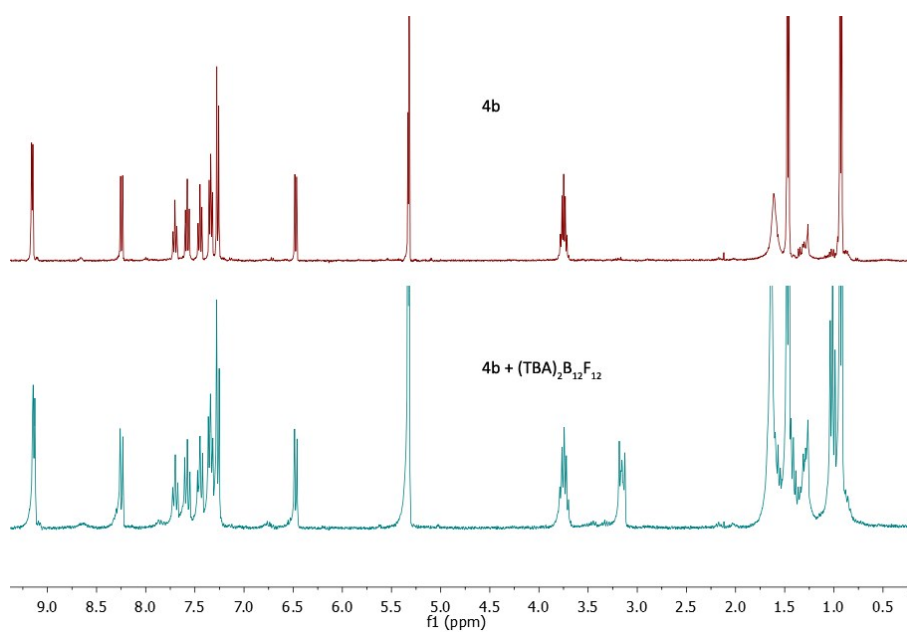


Figure S27 ^1H NMR spectra of model compound **4b** (top) and model compound **4b** in presence of $(\text{TBA})_2\text{B}_{12}\text{F}_{12}$ (bottom) in CD_2Cl_2 at room temperature.

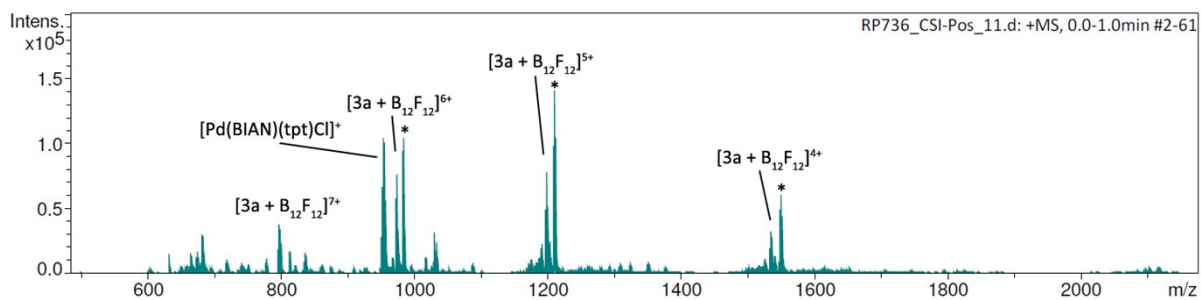


Figure S28 UHR CSI-TOF mass spectrum of **3a** + B₁₂F₁₂ {[Pd₆(BIAN)₆(tpt)₄(B₁₂F₁₂)](OTf)₁₀}. Asterisks indicate BIAN-Pd cage with 2 equivalents B₁₂F₁₂²⁻. These species are proposedly formed during the MS mearurement, with B₁₂F₁₂²⁻ also being able to function as a counterion. Additionally, a fragment with composition ([Pd(BIAN)(tpt)Cl]⁺) can be discerned, indicating of cage decomposition, which results in release of the accompanying B₁₂F₁₂²⁻ guest.

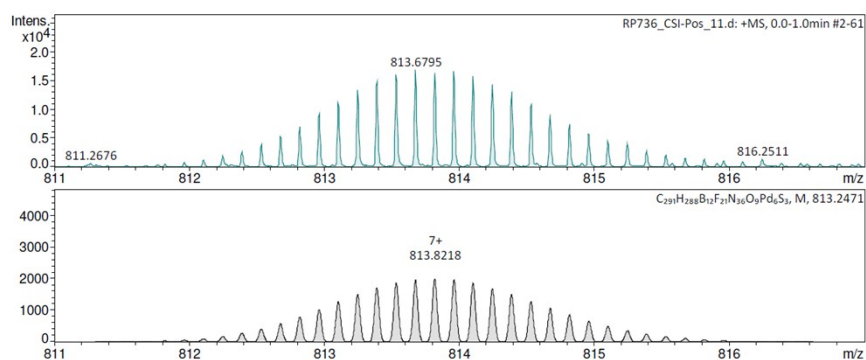


Figure S29 UHR CSI-TOF mass spectrum of Pd(BIAN) cage + B₁₂F₁₂ {[Pd₆(BIAN)₆(tpt)₄(B₁₂F₁₂)](OTf)₃}.

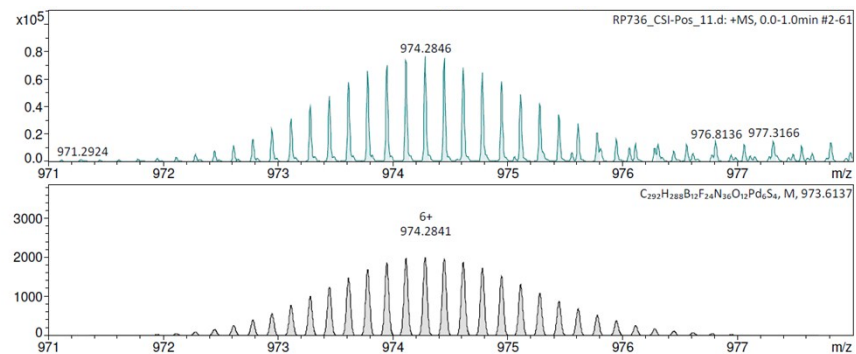


Figure S30 UHR CSI-TOF mass spectrum of **3a** + B₁₂F₁₂ {[Pd₆(BIAN)₆(tpt)₄(B₁₂F₁₂)](OTf)₄}.

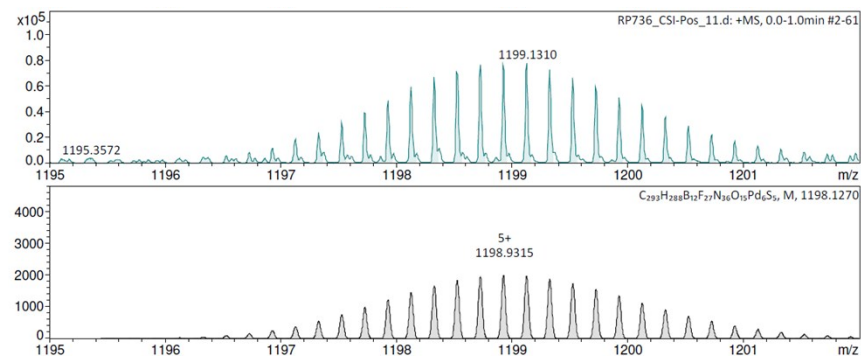


Figure S31 UHR CSI-TOF mass spectrum of **3a** + B₁₂F₁₂ {[Pd₆(BIAN)₆(tpt)₄(B₁₂F₁₂)](OTf)₅}.

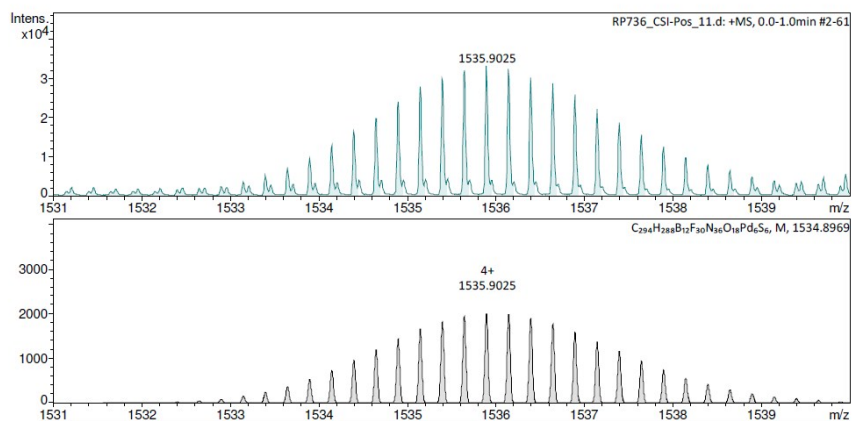


Figure S32 UHR CSI-TOF mass spectrum of **3a** + B₁₂F₁₂ {[Pd₆(BIAN)₆(tpt)₄(B₁₂F₁₂)](OTf)₆}.

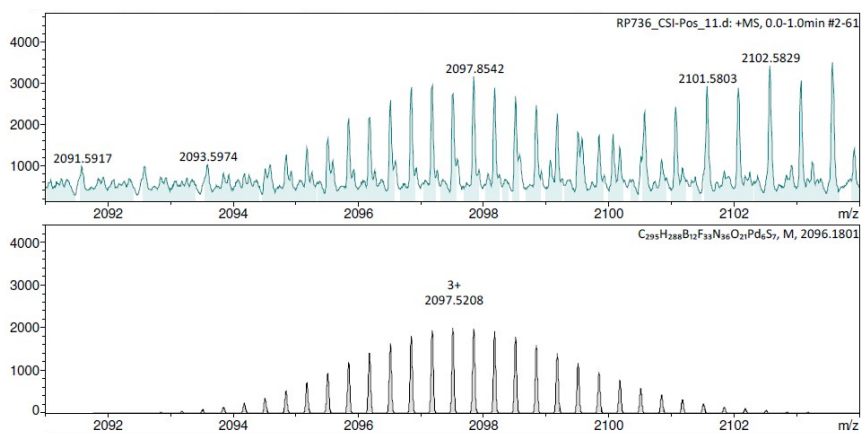


Figure S33 UHR CSI-TOF mass spectrum of **3a** + B₁₂F₁₂ {[Pd₆(BIAN)₆(tpt)₄(B₁₂F₁₂)](OTf)₇}.

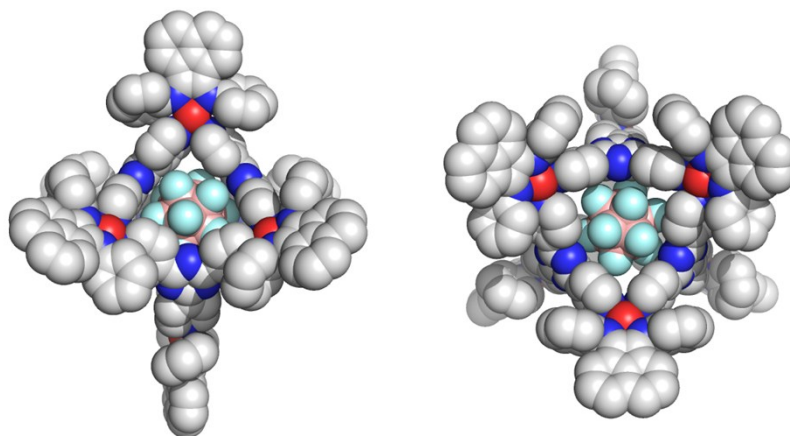


Figure S34 MMFF Models of encapsulated B₁₂F₁₂²⁻ inside BIAN-Pd cage **3a**, showing that only a single guest fits inside the cavity.

Single Crystal X-Ray Diffraction (SC-XRD)

X-ray intensities were measured on a Bruker D8 Quest Eco diffractometer equipped with a Triumph monochromator ($\lambda = 0.71073 \text{ \AA}$) and a CMOS Photon 100 detector at a temperature of 150(2) K. Intensity data were integrated with the Bruker APEX2 software.⁵⁷ Absorption correction and scaling was performed with SADABS.⁵⁸ The structures were solved using intrinsic phasing with the program SHELXT.⁵⁹ Least-squares refinement was performed with SHELXL-2013⁵¹⁰ against F^2 of all reflections. Non-hydrogen atoms were refined with anisotropic displacement parameters. The H atoms were placed at calculated positions using the instructions AFIX 13, AFIX 43 or AFIX 137 with isotropic displacement parameters having values 1.2 or 1.5 times U_{eq} of the attached C atoms. Both complexes **4a** and **4b** were crystallized by vapour diffusion of pentane into a CH_2Cl_2 solution. CCDC 1923049 and 1923050 contain the supplementary crystallographic data for this paper. These data can be obtained free of charge from The Cambridge Crystallographic Data Centre via www.ccdc.cam.ac.uk/data_request/cif.

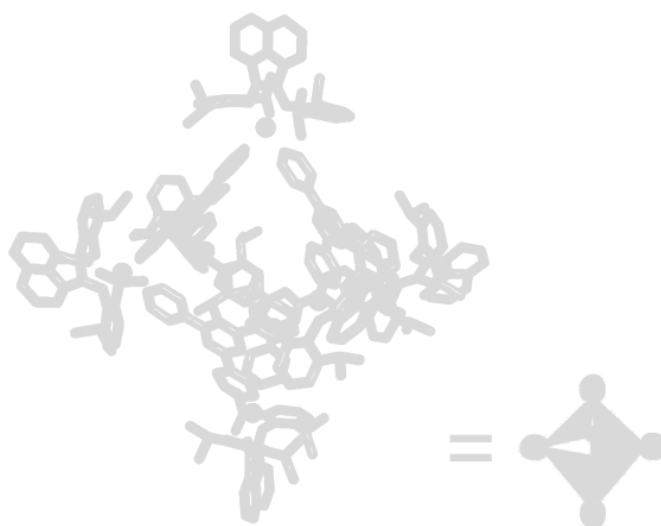


Figure S35 Connectivity plot of **3a**, obtained from X-ray diffraction. Solvent, counterions and hydrogens are omitted for clarity. Pd = red, carbon = grey, nitrogen = blue.

complex 4a: $\text{C}_{49}\text{H}_{52}\text{Cl}_2\text{F}_6\text{N}_4\text{O}_6\text{PdS}_2$, Fw = 1148.36, red-brown block, 0.514×0.281×0.232 mm, triclinic, $P\text{Error!}(\text{No: } 2)$, $a = 11.3214(4)$, $b = 12.0761(5)$, $c = 23.4333(9) \text{ \AA}$, $\alpha = 90.3230(3)$, $\beta = 103.5790(10)$, $\gamma = 116.2730(10)^\circ$, $V = 2770.35(19) \text{ \AA}^3$, $Z = 2$, $D_x = 1.377 \text{ g/cm}^3$, $\mu = 0.575 \text{ mm}^{-1}$. 86029 Reflections were measured up to a resolution of $(\sin \theta/\lambda)_{\text{max}} = 0.84 \text{ \AA}^{-1}$. 9767 Reflections were unique ($R_{\text{int}} = 0.0257$), of which 9045 were observed [$I > 2\sigma(I)$]. 862 Parameters were refined with 861 restraints. $R1/wR2$ [$I > 2\sigma(I)$]: 0.0292/0.0708. $R1/wR2$ [all refl.]: 0.0325/ 0.0729. $S = 1.050$. Residual electron density between -0.620 and 0.666 e/\AA^3 . CCDC 1923049.

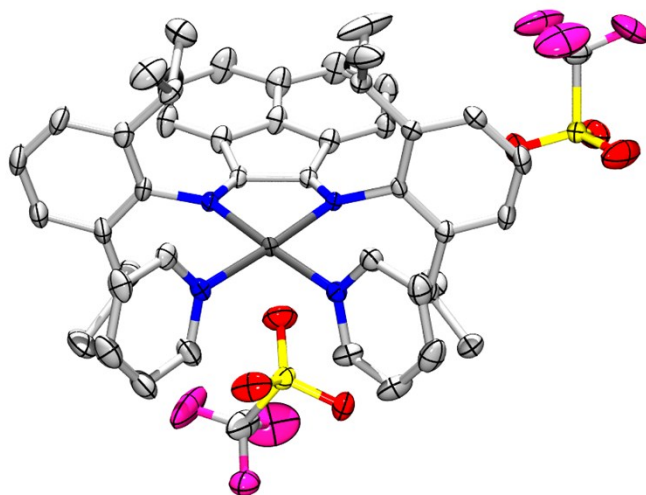


Figure S36 Displacement ellipsoid plot (50% probability level) of [Pd(BIAN)(pyr)₂](OTf)₂. Hydrogen atoms omitted for clarity.

complex 4b: C_{49.5}H₅₃Cl₃F₆N₄O₆PtS₂, Fw = 1279.52, brown block, 0.255×0.128×0.096 mm, monoclinic, C2/c (No: 15), a = 40.579(2), b = 12.5401(7), c = 24.3030(13) Å, β = 121.629(2)°, V = 10530.0(10) Å³, Z = 8, D_x = 1.614 g/cm³, μ = 2.969 mm⁻¹. 197535 Reflections were measured up to a resolution of (sin θ/λ)_{max} = 0.77 Å⁻¹. 12102 Reflections were unique (R_{int} = 0.0512), of which 10264 were observed [I > 2σ(I)]. 669 Parameters were refined with 16 restraints. R1/wR2 [I > 2σ(I)]: 0.0280/0.0517. R1/wR2 [all refl.]: 0.0390/ 0.0551. S = 1.057. Residual electron density between -1.062 and 1.126 e/Å³. CCDC 1923050.

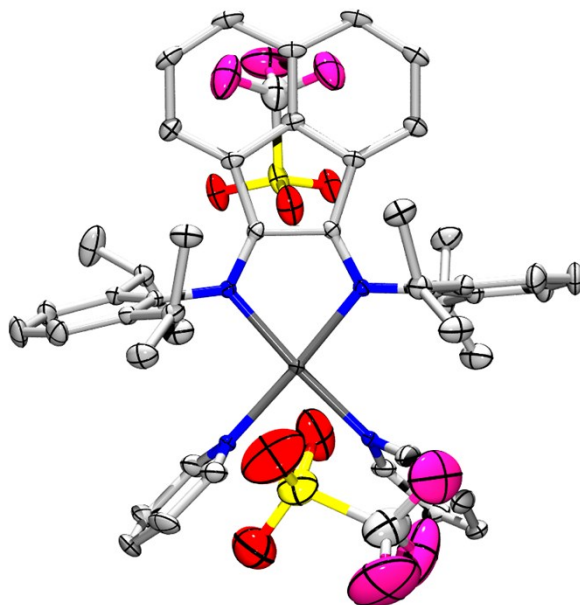


Figure S37 Displacement ellipsoid plot (50% probability level) of [Pt(BIAN)(pyr)₂](OTf)₂. Hydrogen atoms and CH₂Cl₂ lattice solvent molecules omitted for clarity.

Electrochemical Measurements

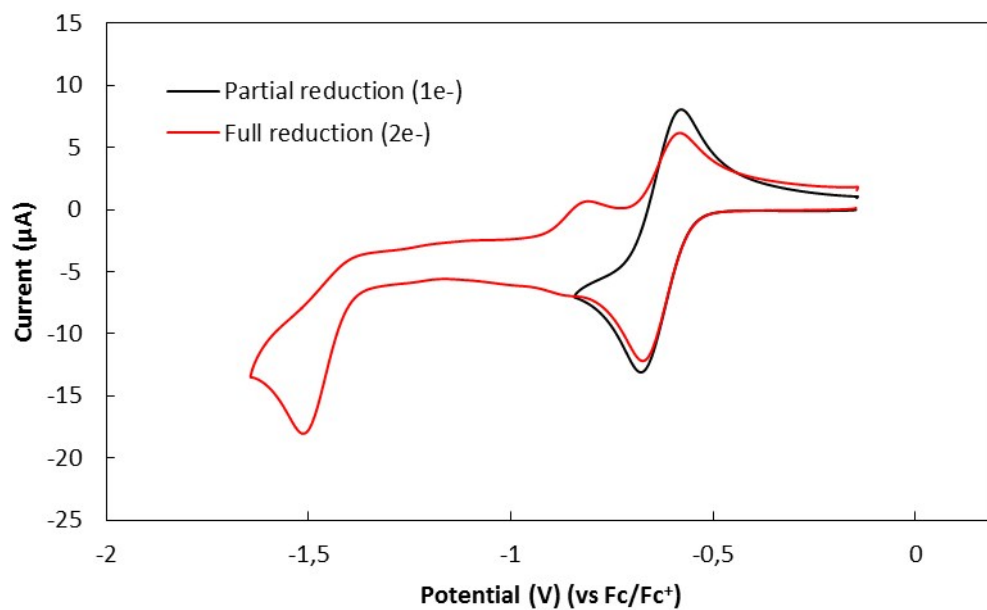


Figure S38 Cyclic voltammogram of **4a** upon scanning to -0.85 V (black line) and to -1.6 V (red line) in CH₂Cl₂ at 100 mV/s.

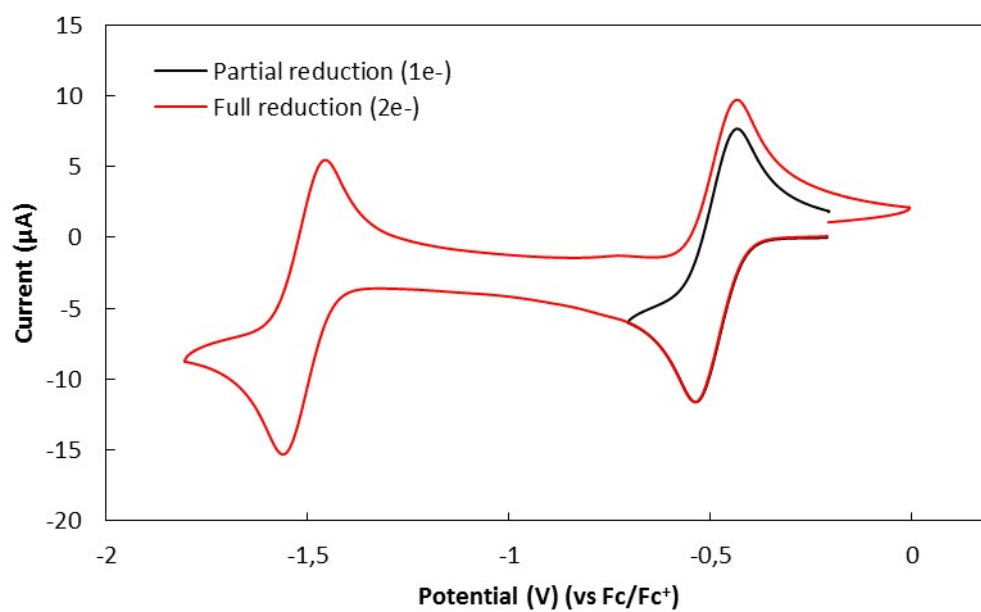


Figure S39 Cyclic voltammogram of **4b** upon scanning to -0.7 V (black line) and to -1.8 V (red line) in CH₂Cl₂ at 100 mV/s.

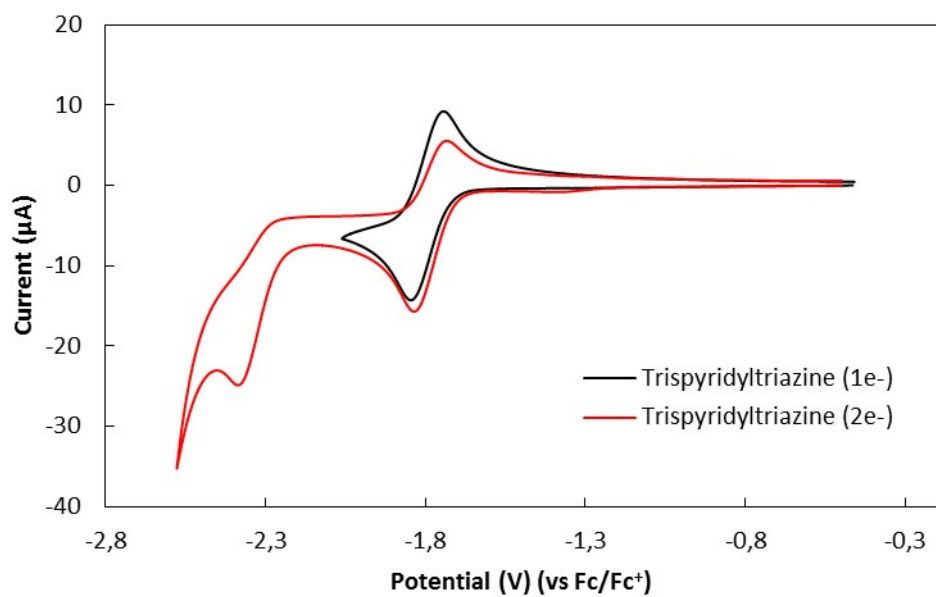


Figure S40 Cyclic voltammogram of trispyridyltriazine (**tpt**) in CH_2Cl_2 at 100 mV/s, reducing the compound by one electron (black line) and by two electrons (red line).

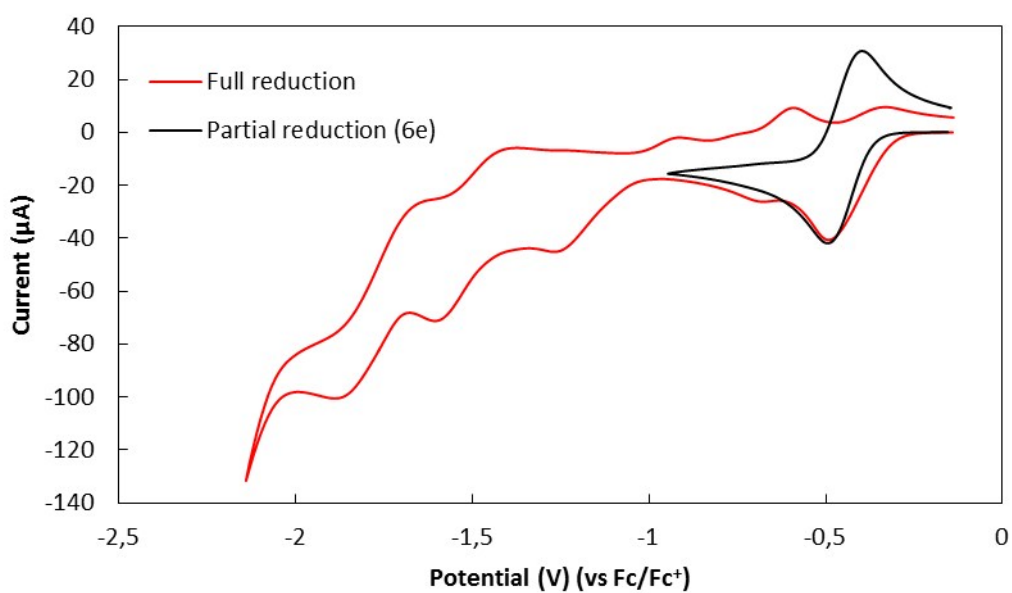


Figure S41 Cyclic voltammogram of **3a** upon scanning to -1.0 V (black line) and to -2.2 V (red line) in CH_2Cl_2 at 100 mV/s.

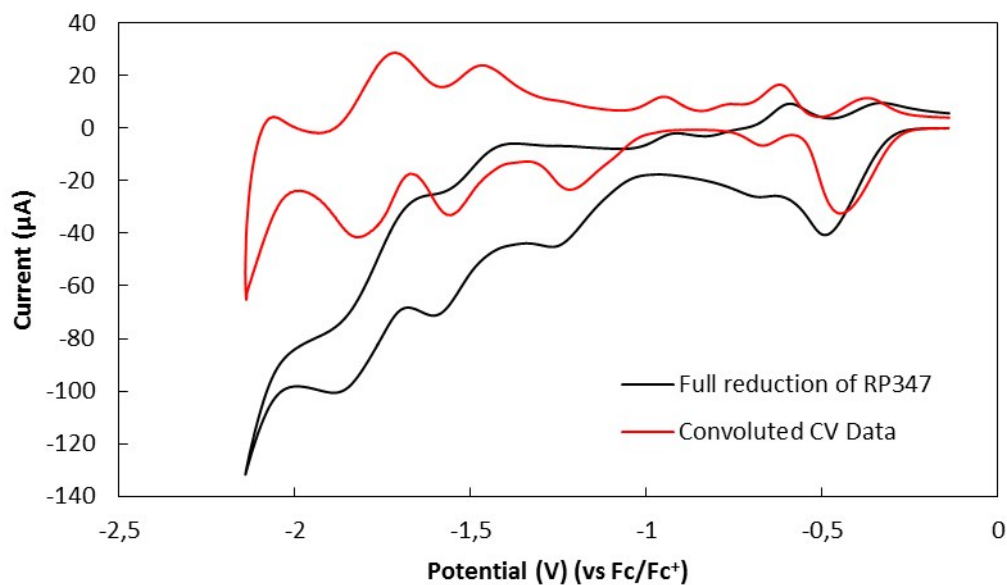


Figure S42 Cyclic voltammogram (black line) of **3a** (black line) and its semi-derivative convolution plot (red line) upon scanning to -2.2 V in CH₂Cl₂ at 100 mV/s.

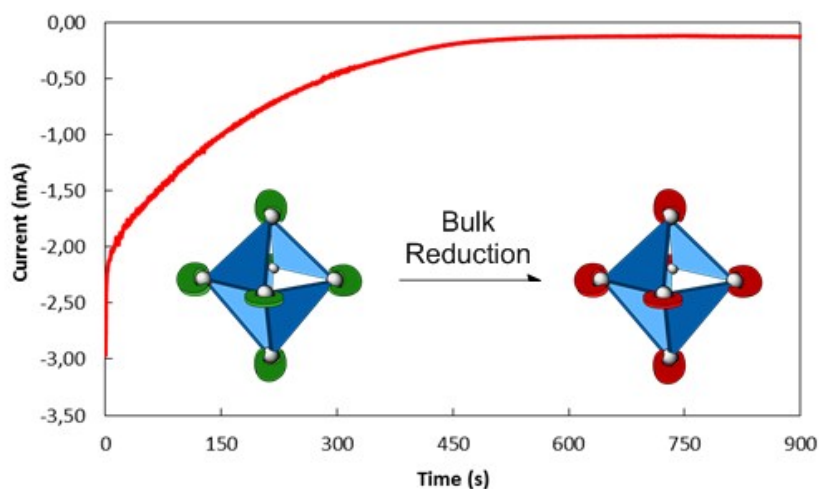


Figure S43 Coulometry measurement of the first reduction wave of the BIAN-cornerstones in cage **3a**. The data is integrated until 600 s. Conditions: 5 mg of **3a** in the working electrode compartment was used. An excess of ferrocene in the counter electrode compartment was used. A cyclic voltammogram was performed prior to bulk electrolysis, after which a fixed potential was set ~200mV over the first redox wave. All bulk electrolysis were performed in DCM using 0.2 M N(*n*-Bu)₄PF₆ as supporting electrolyte.

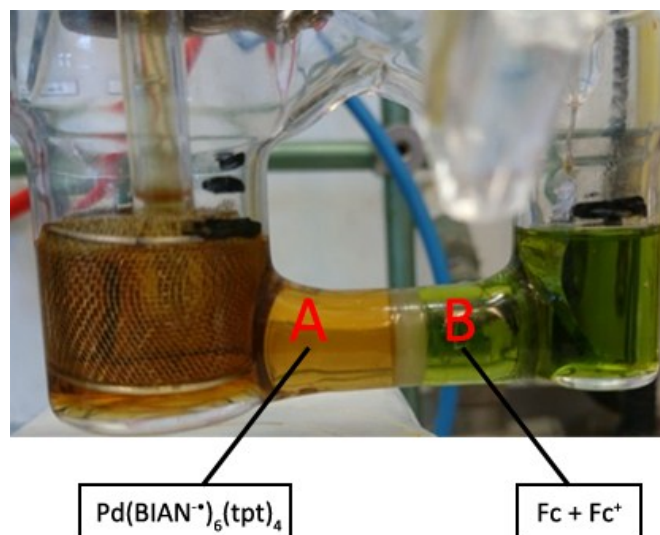


Figure S44 Photograph of the bulk electrolysis set-up; compartment A contains the working- and reference-electrode (Pt-mesh and Ag-wire, respectively) and the compartment B contains the counter electrode (Pt-sheet) and a sacrificial electron donor (ferrocene).

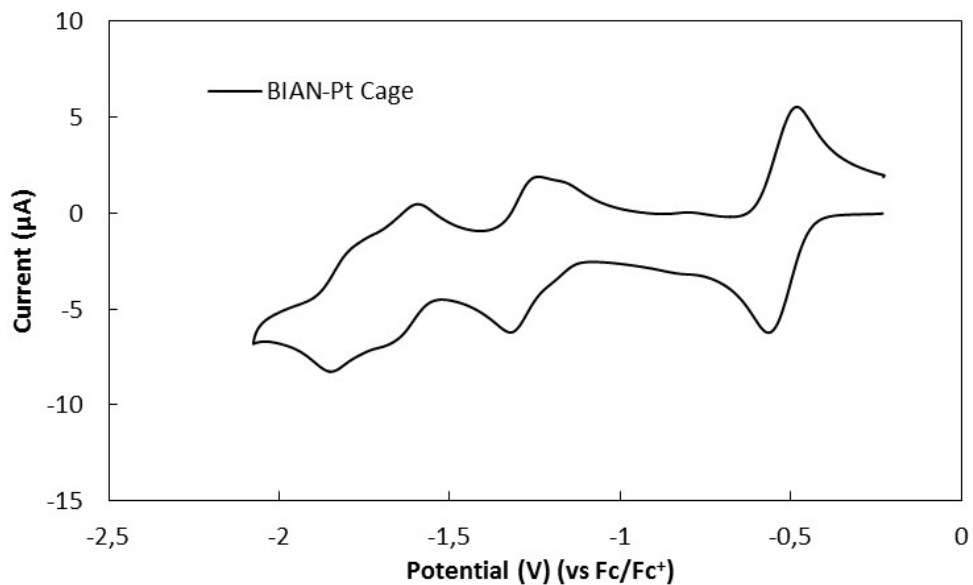


Figure S45 Cyclic voltammogram of **3b** in CH_2Cl_2 at 100 mV/s.

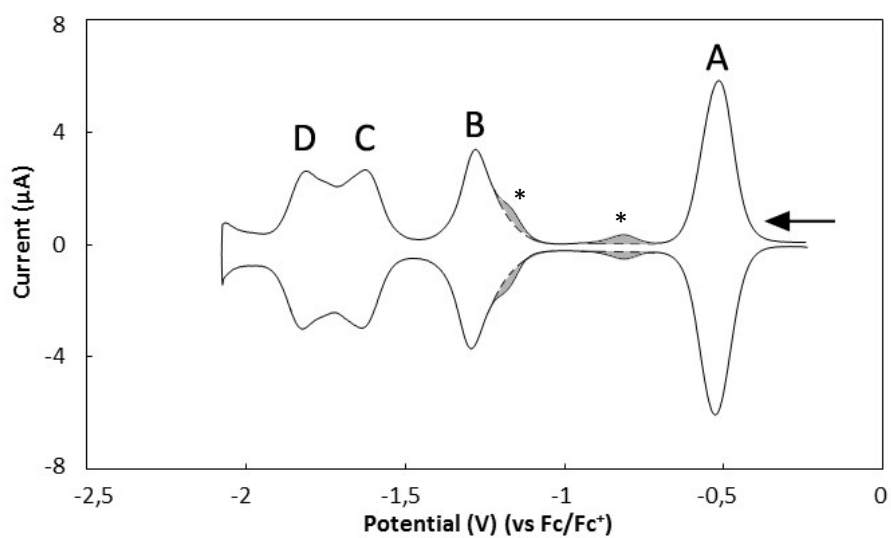


Figure S46 Semi-derivative convolution plot of CV of **3b** in CH_2Cl_2 at 100 mV/s, showing full reversibility. Individual reduction processes are numbered above the waves (A-D). Minor impurity (~3%) indicated by (*).

Ultra-high Resolution Cryospray-ionization Mass Measurements

Cryospray-ionization MS (CSI-MS) measurements were performed on a UHR-TOF Bruker Daltonik maXis plus, an ESI-quadrupole time-of-flight (qToF) mass spectrometer capable of a resolution of at least 60,000 (FWHM), which was coupled to a Bruker Daltonik Cryospray unit.

Detection was in positive ion mode, the source voltage was 4.2 kV. The flow rates were 220 $\mu\text{L}/\text{hour}$. The drying gas (N_2), to aid solvent removal, was held at $-35\text{ }^\circ\text{C}$ and the spray gas was held at $-40\text{ }^\circ\text{C}$.

The machine was calibrated prior to every experiment via direct infusion of the Agilent ESI-TOF low concentration tuning mixture, which provided an m/z range of singly charged peaks up to 2700 Da in both ion modes.

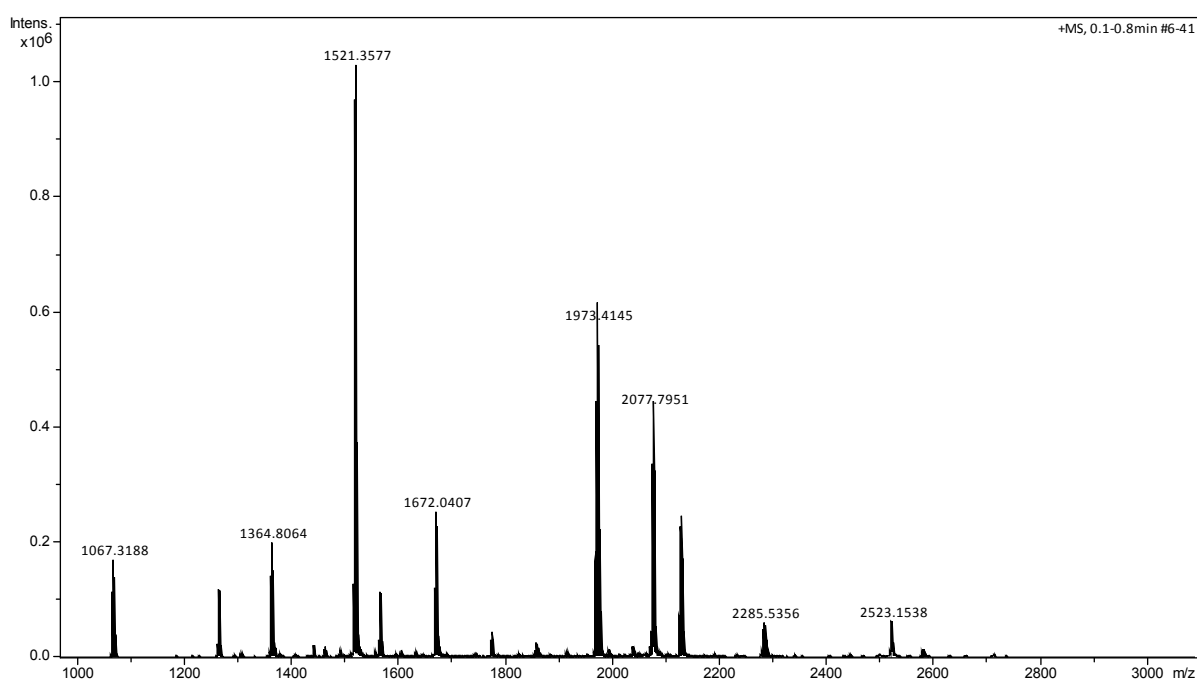


Figure S47 UHR CSI-MS mass spectrum of **3a** with a spray temperature of $-40\text{ }^\circ\text{C}$ and a dry gas temperature of $-35\text{ }^\circ\text{C}$.

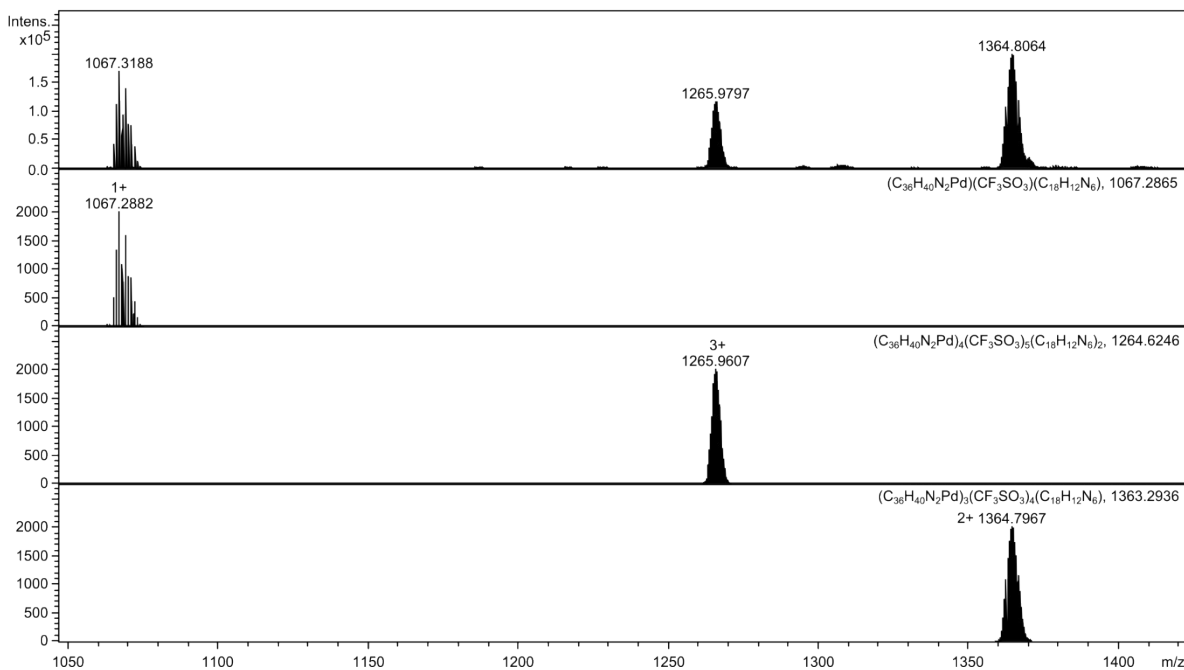


Figure S48 UHR CSI-MS mass spectrum of (top) $[\text{Pd}(\text{BIAN})(\text{tpt})](\text{OTf})^{1+}$, $[\text{Pd}_4(\text{BIAN})_4(\text{tpt})_2](\text{OTf})_5^{3+}$ and $[\text{Pd}_3(\text{BIAN})_3(\text{tpt})_2](\text{OTf})_4^{2+}$, respectively, and below) simulated isotopic distributions with a spray temperature of -40°C and a dry gas temperature of -35°C .

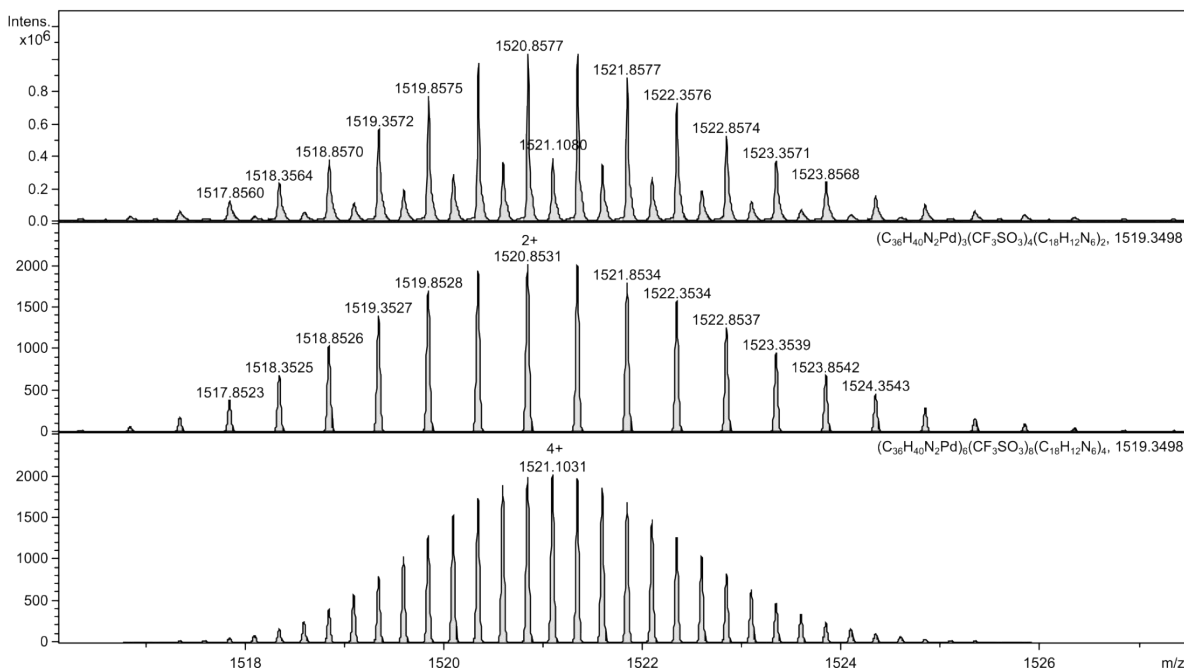


Figure S49 UHR CSI-MS mass spectrum of (top) $[\text{Pd}_3(\text{BIAN})_3(\text{tpt})_2](\text{OTf})_4^{2+}$ and $[\text{Pd}_6(\text{BIAN})_6(\text{tpt})_4](\text{OTf})_8^{4+}$ and below) simulated isotopic distribution with a spray temperature of -40°C and a dry gas temperature of -35°C .

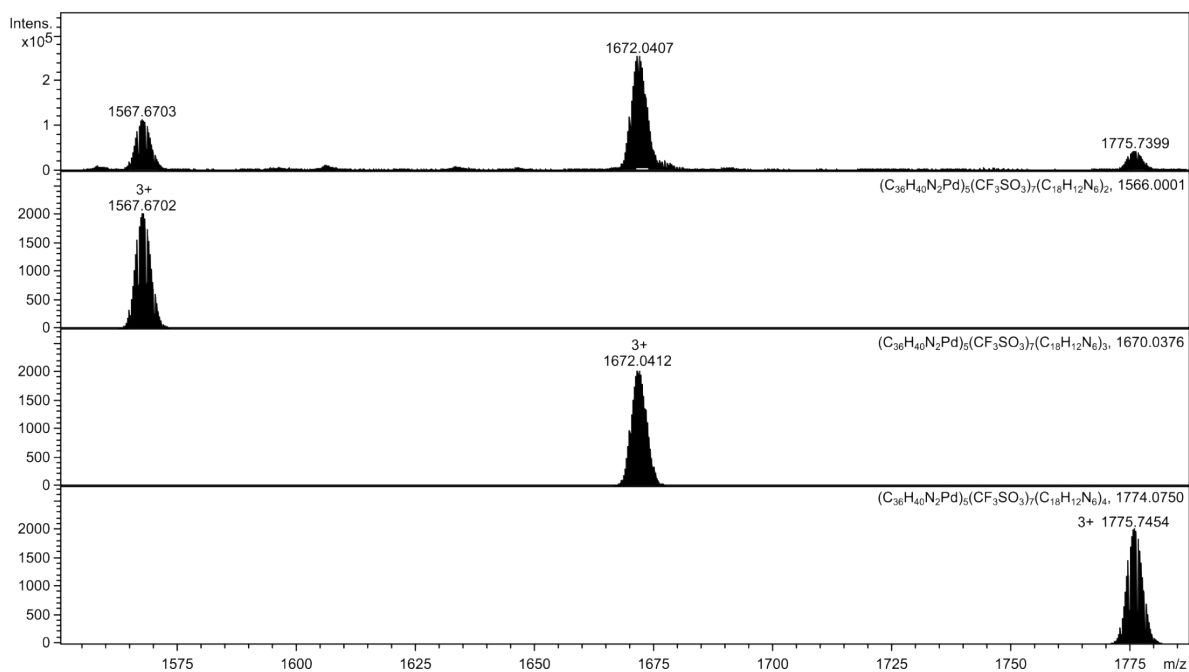


Figure S50 UHR CSI-MS mass spectrum of (top) $[\text{Pd}_5(\text{BIAN})_5(\text{tpt})_2](\text{OTf})_7^{3+}$, $[\text{Pd}_5(\text{BIAN})_5(\text{tpt})_3](\text{OTf})_7^{3+}$ and $[\text{Pd}_5(\text{BIAN})_5(\text{tpt})_4](\text{OTf})_7^{3+}$ and (below) simulated isotopic distribution with a spray temperature of $-40\text{ }^\circ\text{C}$ and a dry gas temperature of $-35\text{ }^\circ\text{C}$.

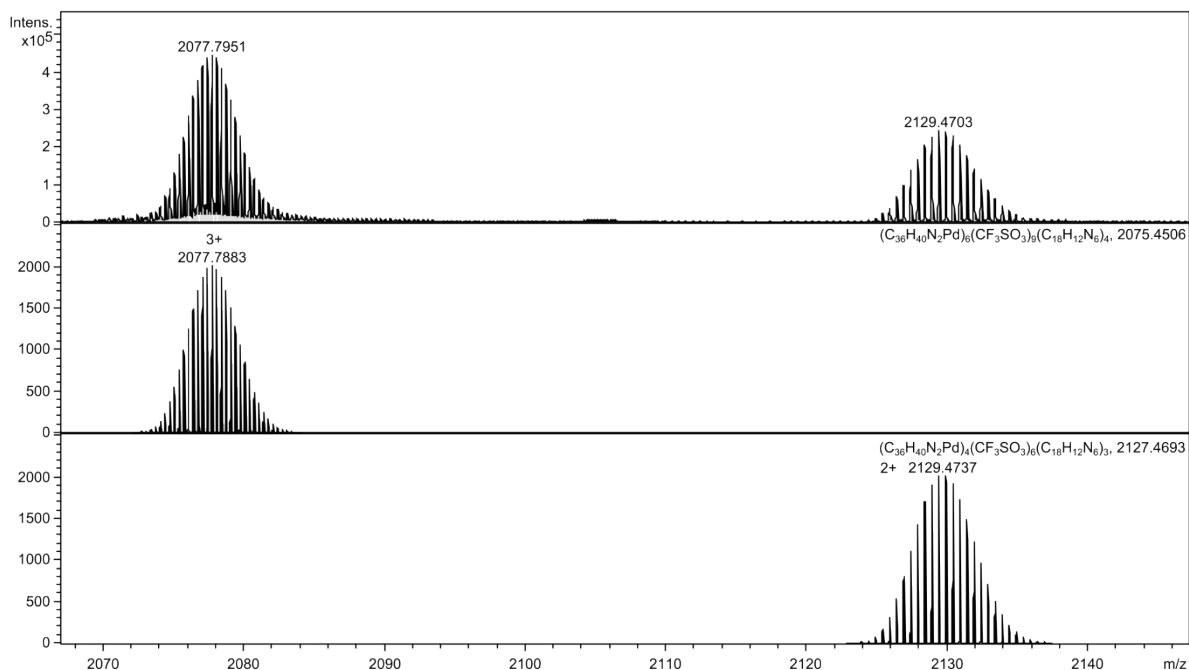


Figure S51 UHR CSI-MS mass spectrum of (top) $[\text{Pd}_6(\text{BIAN})_6(\text{tpt})_4](\text{OTf})_9^{3+}$ and $[\text{Pd}_4(\text{BIAN})_4(\text{tpt})_3](\text{OTf})_6^{2+}$, and (below) simulated isotopic distribution with a spray temperature of $-40\text{ }^\circ\text{C}$ and a dry gas temperature of $-35\text{ }^\circ\text{C}$.

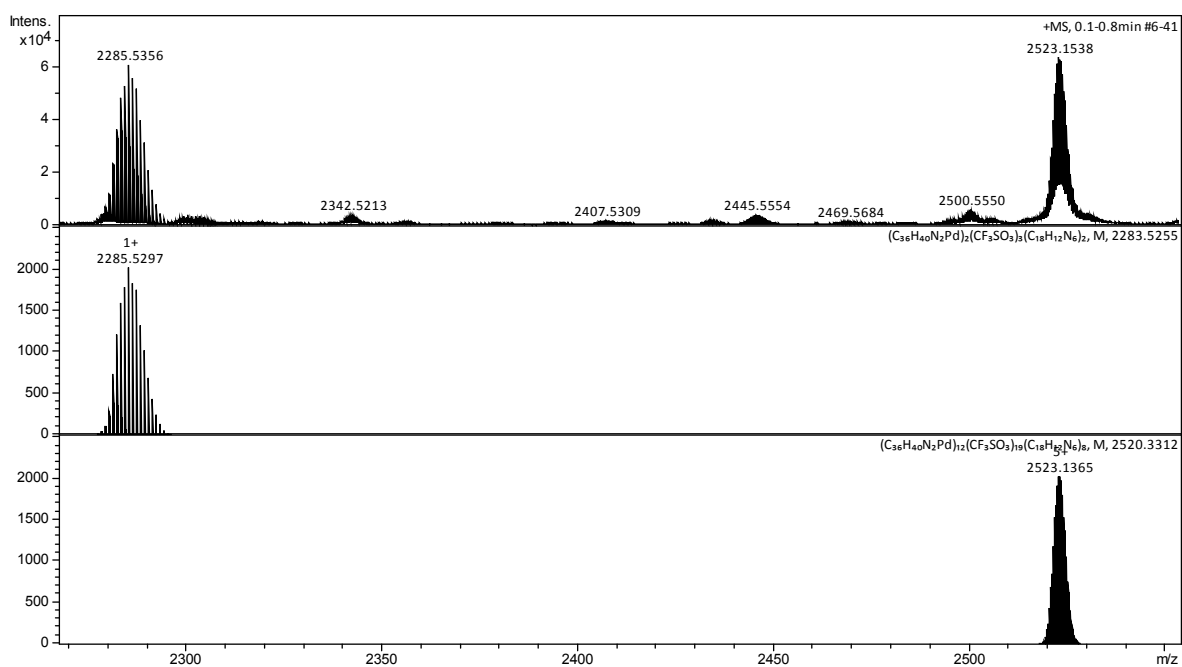


Figure S52 UHR CSI-MS mass spectrum of (top) $[\text{Pd}_2(\text{BIAN})_2(\text{tpt})_2](\text{OTf})_3^{1+}$ and $[\text{Pd}_{12}(\text{BIAN})_{12}(\text{tpt})_8](\text{OTf})_{19}^{5+}$, and (below) simulated isotopic distribution with a spray temperature of $-40\text{ }^\circ\text{C}$ and a dry gas temperature of $-35\text{ }^\circ\text{C}$.

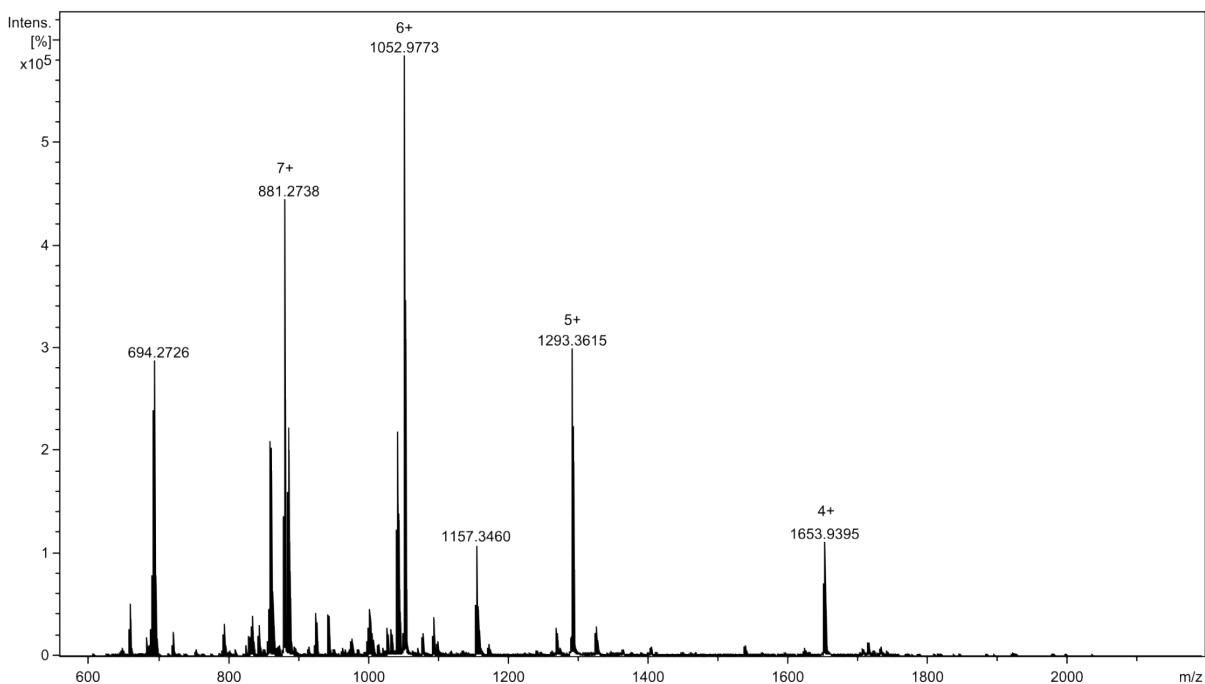


Figure S53 UHR CSI-MS mass spectrum of **3b** with a spray temperature of $-40\text{ }^\circ\text{C}$ and a dry gas temperature of $-35\text{ }^\circ\text{C}$.

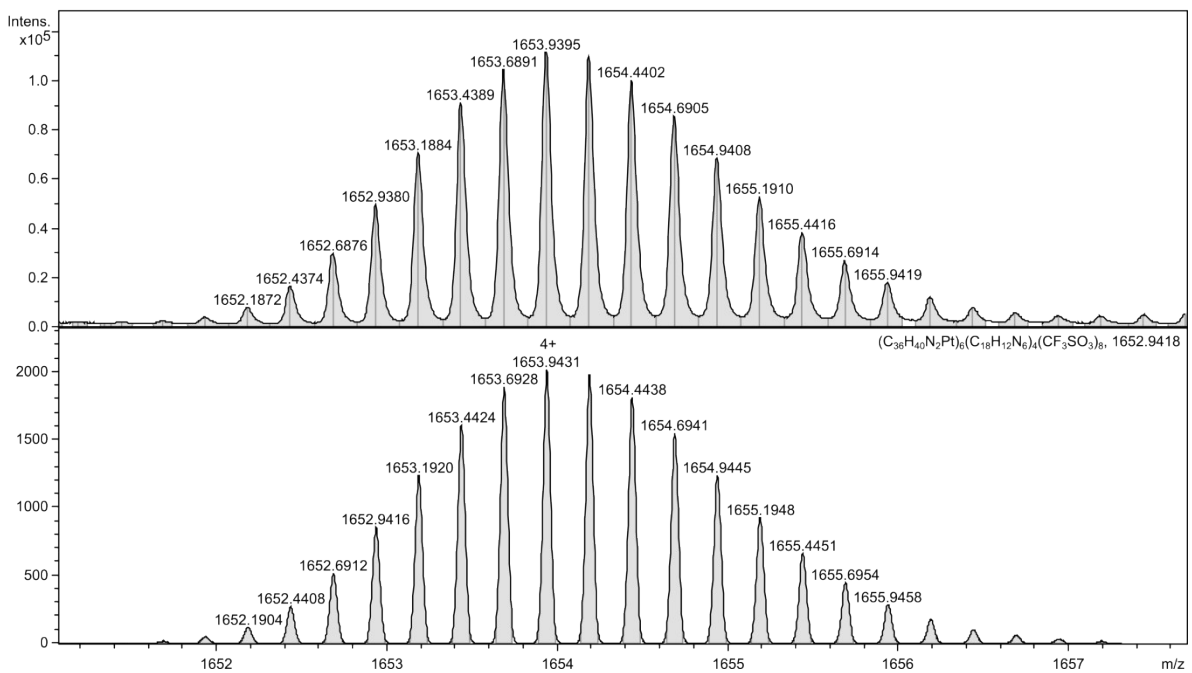


Figure S54 UHR CSI-MS mass spectrum of (top) $[\text{Pt}_6(\text{BIAN})_6(\text{tpt})_4](\text{OTf})_8^{4+}$, and (below) simulated isotopic distribution with a spray temperature of -40°C and a dry gas temperature of -35°C .

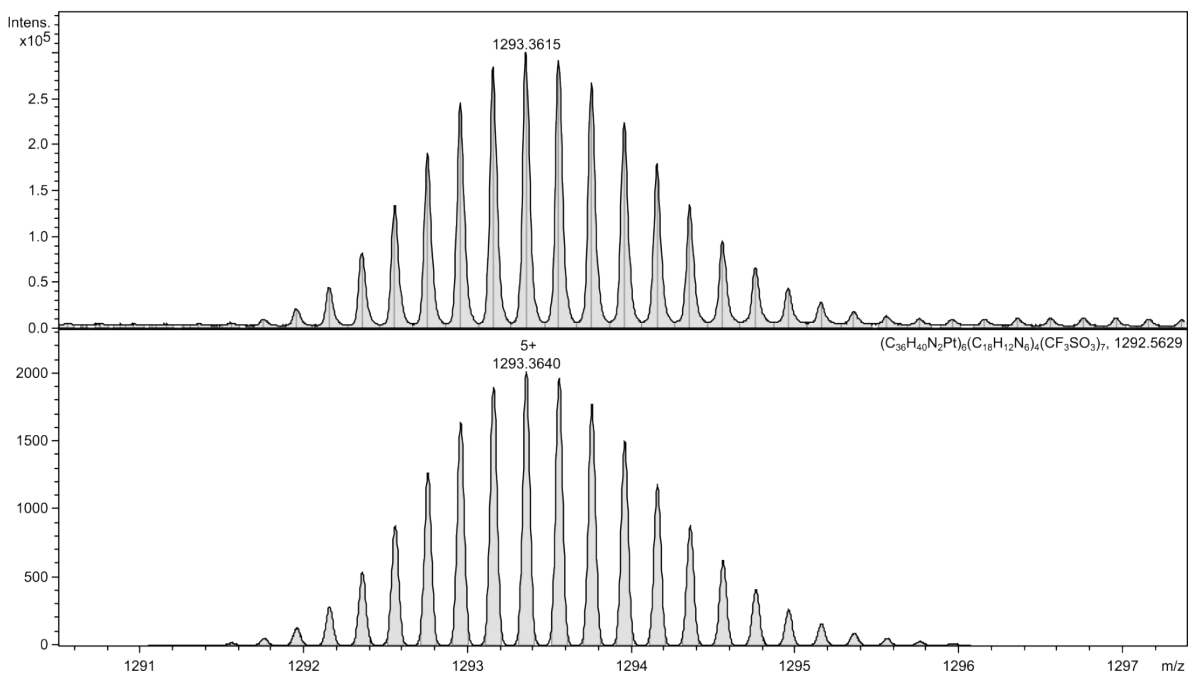


Figure S55 UHR CSI-MS mass spectrum of (top) $[\text{Pt}_6(\text{BIAN})_6(\text{tpt})_4](\text{OTf})_7^{5+}$, and (below) simulated isotopic distribution with a spray temperature of -40°C and a dry gas temperature of -35°C .

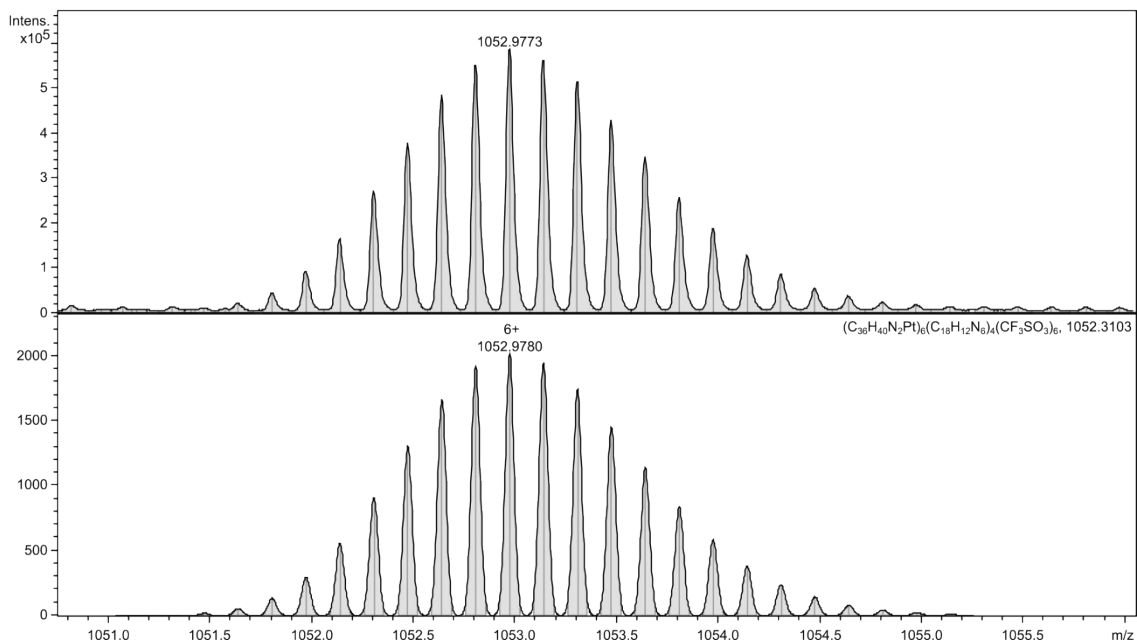


Figure S56 UHR CSI-MS mass spectrum of (top) $[\text{Pt}_6(\text{BIAN})_6(\text{tpt})_4](\text{OTf})_6^{6+}$, and (below) simulated isotopic distribution with a spray temperature of $-40\text{ }^\circ\text{C}$ and a dry gas temperature of $-35\text{ }^\circ\text{C}$.

Electron Paramagnetic Resonance (EPR)

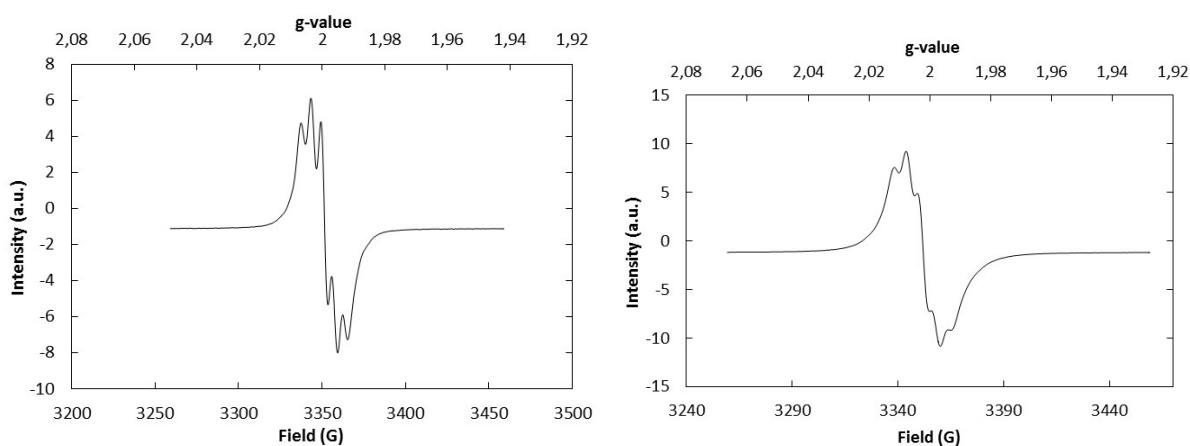


Figure S57 EPR spectrum of model system **4a** upon chemical reduction with 1 equivalent of CoCp_2 (left) and **3a** upon chemical reduction with 6 equivalents of CoCp_2 (right) both measured at room temperature in CH_2Cl_2 .

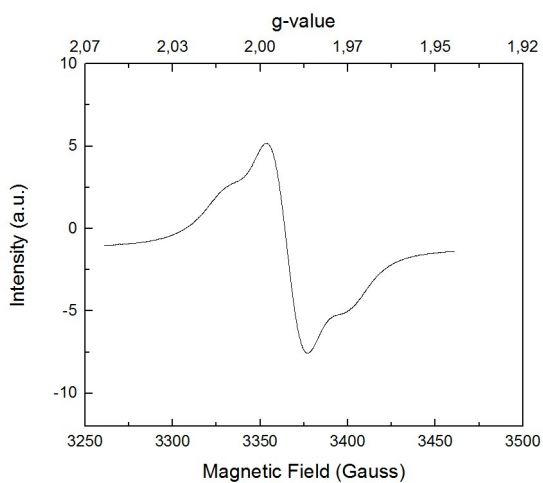


Figure S58 EPR spectrum of model system **4b** upon chemical reduction with 1 equivalent of CoCp_2 measured at room temperature in CH_2Cl_2 .

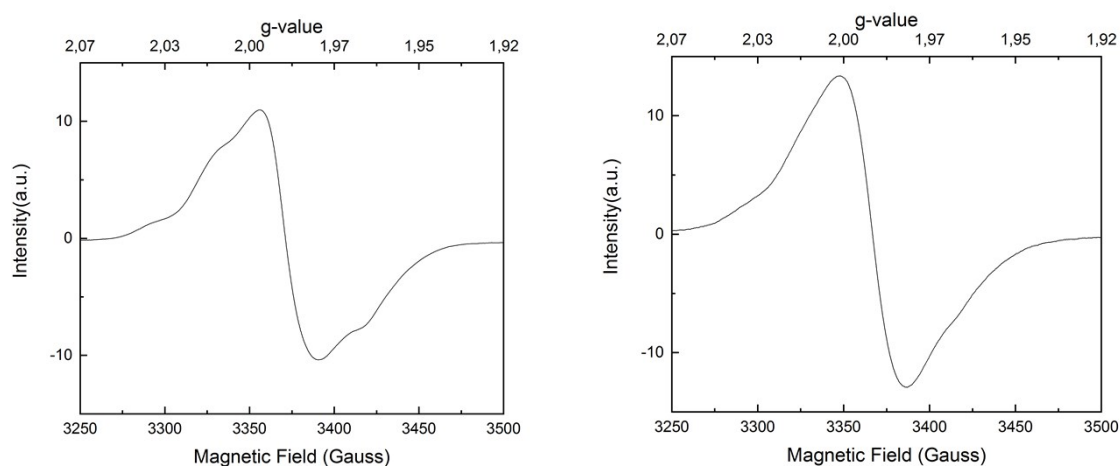


Figure S59 EPR spectrum of **3b** upon cathodic reduction at -1.0 V (left) and -1.5 V (right), both measured at 10 K in frozen CH_2Cl_2 containing $\text{N}(n\text{-Bu}_4)\text{PF}_6$ (0.2 M).

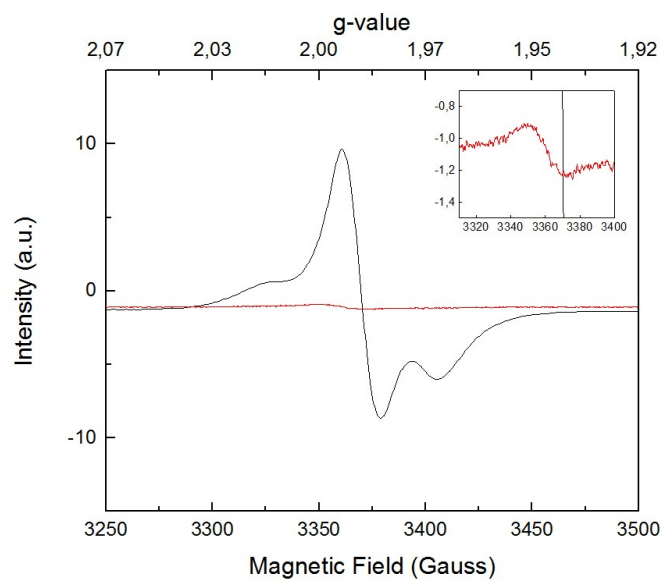


Figure S60 EPR measurements at room temperature of BIAN-Pt cage (**3b**) after selective reduction over the first wave (A) (black) and upon full reduction at -2.0 V vs. Fc/Fc⁺ (red, inset = 38x zoom) using bulk electrolysis.

UV/Vis Spectro-Electrochemistry

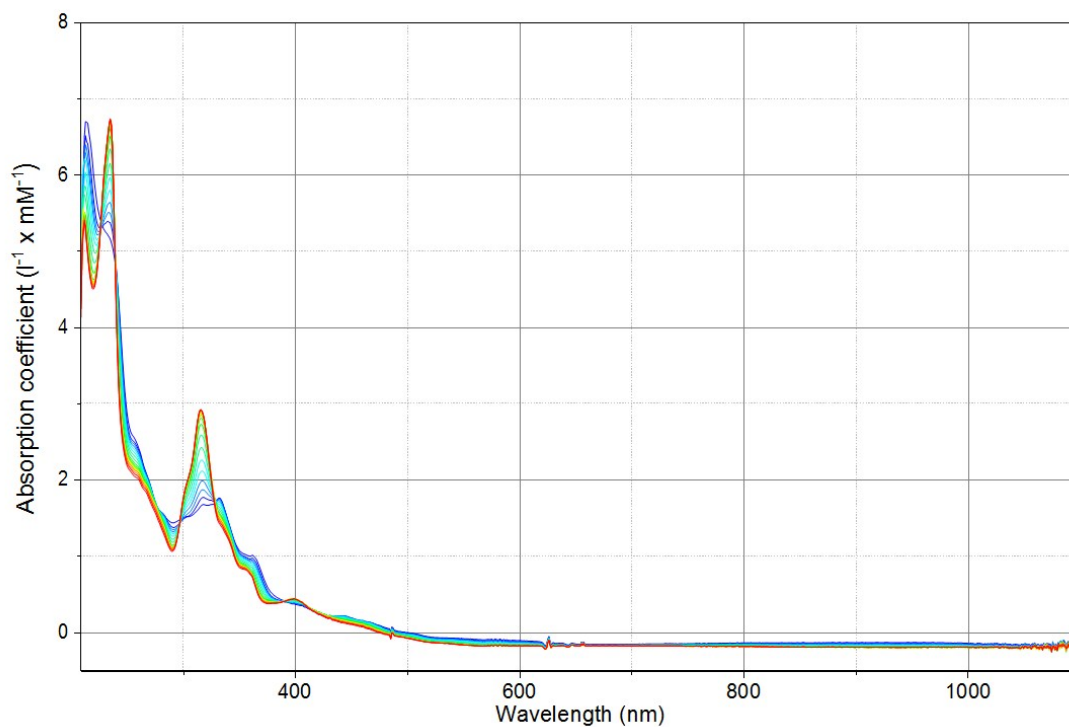


Figure S61 UV/vis-SEC of **4b** upon cathodic reduction at -1.0 V, corresponding to the **adi/aia**[•] redox-couple of the BIAN ligand.

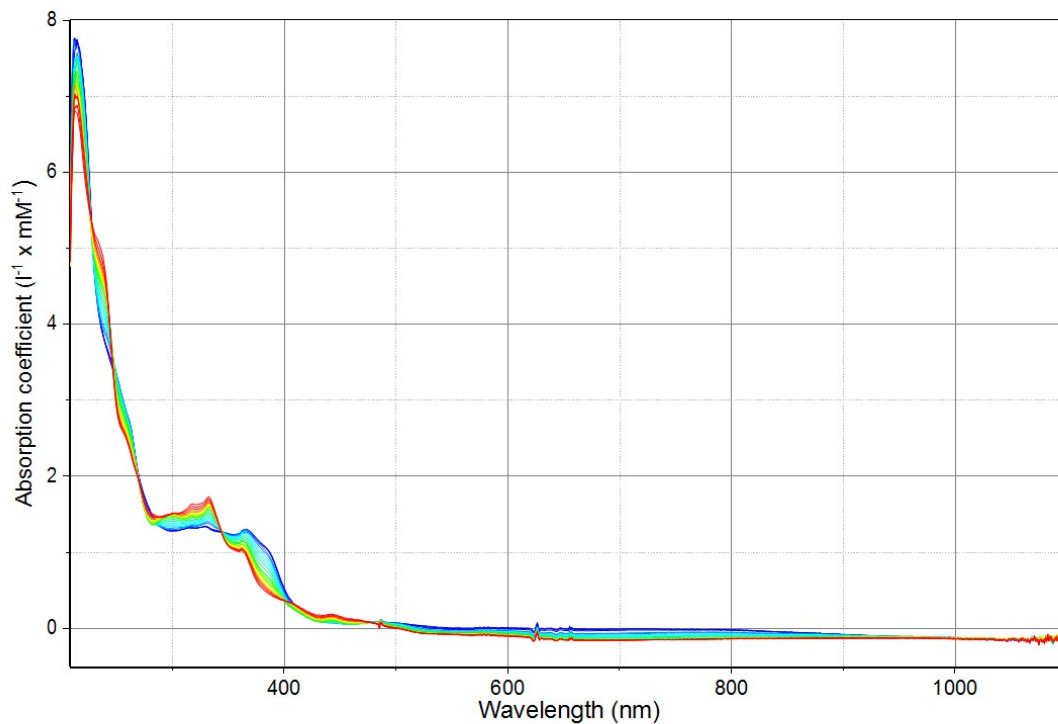


Figure S62 UV/vis-SEC of **4b** upon cathodic reduction at -1.8 V, corresponding to the **aia^{•-}/ada²⁻** redox-couple of the BIAN ligand.

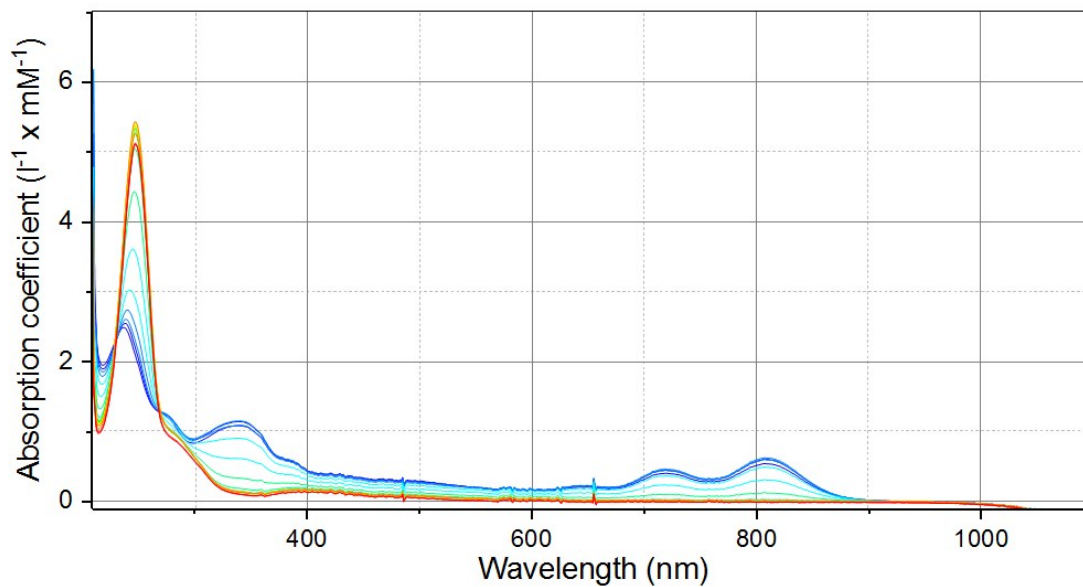


Figure S63 UV/vis-SEC of **tpt** upon cathodic reduction at -2.0 V, corresponding to the **tpt/tpt^{•-}** redox-couple.

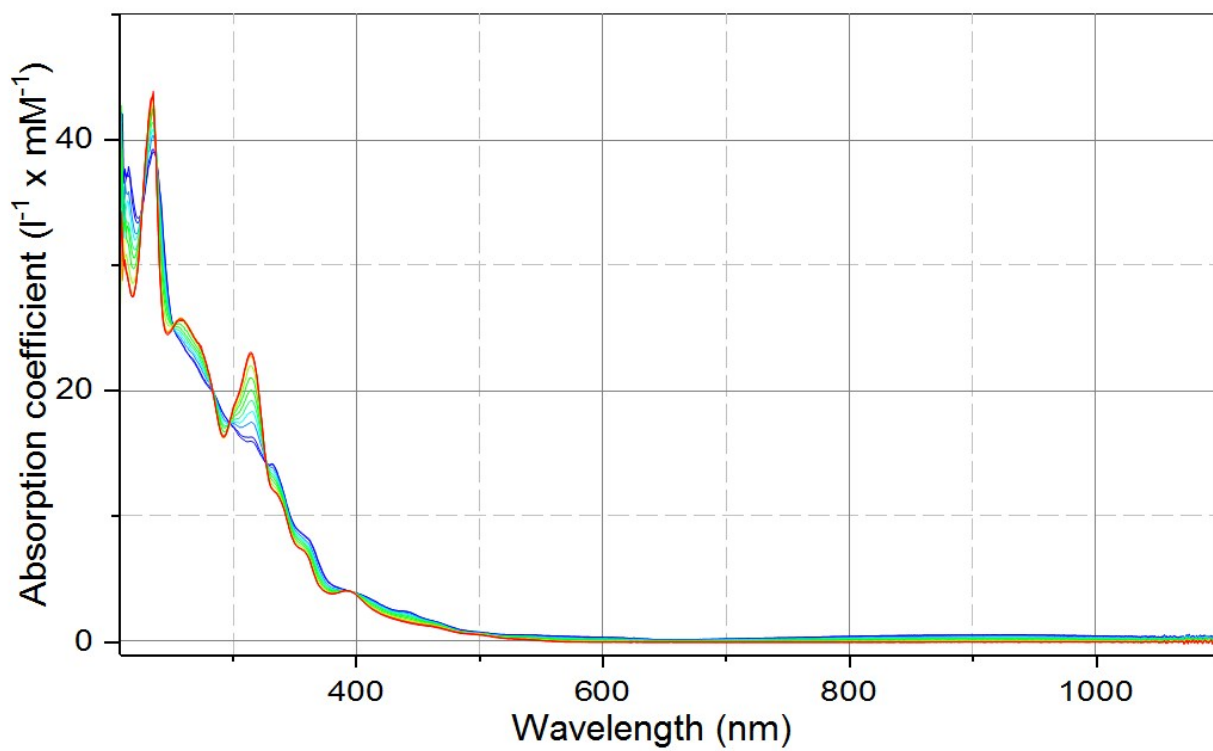


Figure S64 UV/vis-SEC of **3b** upon cathodic reduction at -1.0 V

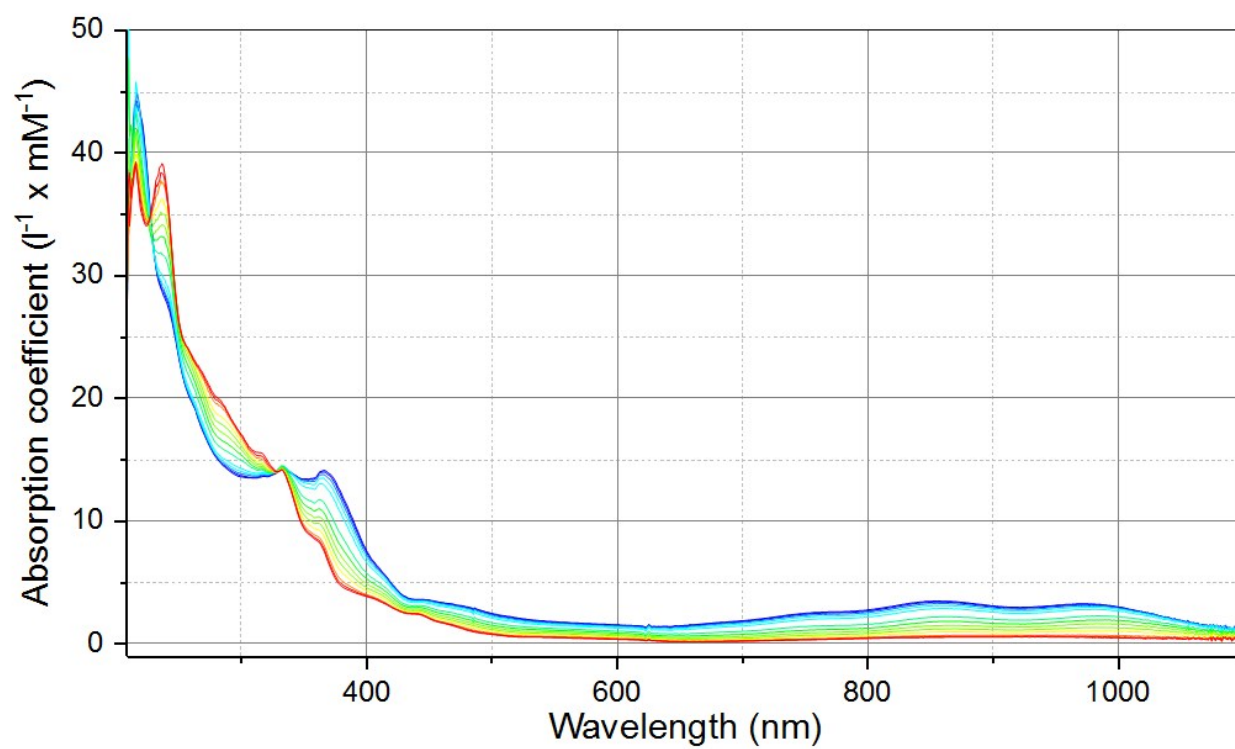


Figure S65 UV/vis-SEC of **3b** upon cathodic reduction at -1.5 V.

References

- (S1) K. R. Harris, *J. Chem. Phys.*, 2009, **131**, 054503.
- (S2) M. Krejčík, M. Daněk and F. Hartl, *J. Electroanal. Chem. Interfacial Electrochem.*, 1991, **317**, 179.
- (S3) S. H. A. M. Leenders, R. Becker, T. Kumpulainen, B. de Bruin, T. Sawada, T. Kato, M. Fujita and J. N. H. Reek, *Chem. Eur. J.*, 2016, **22**, 15468.
- (S4) R. van Asselt, C. J. Elsevier, W. J. J. Smeets, A. L. Spek and R. Benedix, *Recl. Trav. Chim. Pay-B.*, 2010, **113**, 88.
- (S5) R. van Asselt, C. J. Elsevier, C. Amatore and A. Jutand, *Organometallics*, 1997, **16**, 317.
- (S6) Tao,; J. F. Li, A. Q. Peng, X. L. Sun, X. H. Yang and Y. Tang, *Chem. Eur. J.*, 2013, **19**, 13956.
- (S7) R. T. Boéré, J. Derendorf, C. Jenne, S. Kacprzak, M. Keßler, R. Riebau, S. Riedel, T. L. Roemmele, M. Rühle, H. Scherer, T. Vent-Schmidt, J. Warneke, S. Weber, *Chem. Eur. J.*, 2014, **20**, 4447.
- (S7) Bruker, *APEX2* software, Madison WI, USA, 2014.
- (S8) G. M. Sheldrick, *SADABS*, Universität Göttingen, Germany, 2008.
- (S9) G. M. Sheldrick, *Acta Cryst. A*, 2015, **71**, 3.
- S10) G. M. Sheldrick, *SHELXL2013*, University of Göttingen, Germany, 2013.